

1                   **Two cGAS-like receptors induce antiviral immunity in *Drosophila***

2                   Andreas Holleufer<sup>1\*</sup>, Kasper Grønbjerg Winther<sup>2\*</sup>, Hans Henrik Gad<sup>1\*</sup>, Xianlong Ai<sup>3</sup>,  
3                   Yuqiang Chen<sup>3</sup>, Lihua Li<sup>3</sup>, Ziming Wei<sup>3</sup>, Huimin Deng<sup>3</sup>, Jiyong Liu<sup>3</sup>, Ninna Ahlmann  
4                   Frederiksen<sup>1</sup>, Bine Simonsen<sup>1</sup>, Line Lykke Andersen<sup>4</sup>, Karin Kleigrew<sup>5</sup>, Louise Dalskov<sup>1</sup>,  
5                   Andreas Pichlmair<sup>4,6</sup>, Hua Cai<sup>3\*\*</sup>, Jean-Luc Imler<sup>2,3\*\*</sup> and Rune Hartmann<sup>1\*\*</sup>.

6                   **Affiliations:**

7                   <sup>1</sup>Department of Molecular Biology and Genetics, Aarhus University, Aarhus, Denmark.

8                   <sup>2</sup>University of Strasbourg, CNRS UPR9022, Strasbourg, France.

9                   <sup>3</sup>Sino-French Hoffmann Institute, School of Basic Medical Science, Guangzhou Medical  
10                  University, Guangzhou, China.

11                  <sup>4</sup>Institute of Virology, Technical University of Munich, Munich, Germany.

12                  <sup>5</sup>Bavarian Center for Biomolecular Mass Spectrometry, Technical University of Munich,  
13                  Freising, Germany

14                  <sup>6</sup>German Center for Infection Research (DZIF), Munich partner site, Munich, Germany

15                  \* These authors contributed equally to this work.

16                  \*\*Corresponding authors: [chjorbe@hotmail.com](mailto:chjorbe@hotmail.com) (H.C.); [jl.imler@ibmc-cnrs.unistra.fr](mailto:jl.imler@ibmc-cnrs.unistra.fr)  
17                  (J.L.I.); [rh@mbg.au.dk](mailto:rh@mbg.au.dk) (R.H.)

18 **In mammals, cGAS produces the cyclic dinucleotide (CDN) 2'3'-cGAMP in response to**  
19 **cytosolic DNA and this triggers an antiviral immune response. cGAS belongs to a large**  
20 **family of cGAS/DncV-like nucleotidyltransferases, present in both prokaryotes<sup>1</sup> and**  
21 **eukaryotes<sup>2-5</sup>. In bacteria, these enzymes synthesize a range of cyclic oligonucleotide and**  
22 **have emerged as important regulators of phage infections<sup>6-8</sup>. Here, we identify two novel**  
23 **cGAS-like receptors (cGLRs) in the insect *Drosophila melanogaster*. We show that**  
24 **cGLR1 and cGLR2 activate Sting and NF- $\kappa$ B dependent antiviral immunity in response**  
25 **to infection with RNA or DNA viruses. cGLR1 is activated by dsRNA to produce the**  
26 **novel CDN 3'2'-cGAMP whereas cGLR2 produces a combination of 2'3'-cGAMP and**  
27 **3'2' cGAMP in response to a yet unidentified stimulus. Our data establish cGAS as the**  
28 **founding member of a family of receptors sensing different types of nucleic acids and**  
29 **triggering immunity through production of CDNs beyond 2'3'-cGAMP.**

30 Insects represent 65% of all living animal species and host a wide diversity of viruses, yet we  
31 know relatively little about how viral infections are recognized within this group of animals.  
32 The common perception of antiviral immunity in insects has so far been dominated by the  
33 extensive characterization of the RNA interference (RNAi) pathway<sup>9</sup>. However,  
34 transcriptional responses to virus infections have also been identified in the fruit fly  
35 *Drosophila melanogaster*, several genera of mosquitos and other insects. The Toll and  
36 immune deficiency (IMD) pathways, as well as the JAK-STAT pathway, have been proposed  
37 to participate in antiviral defenses, although the exact mechanisms are poorly described<sup>10</sup>. In  
38 addition, we and others recently reported that the signaling adapter Sting participates in  
39 antiviral immunity in *D. melanogaster* as well as the silkworm *Bombyx mori*<sup>11-13</sup>. However,  
40 how virus infections are recognized to induce these pathways in insects remains unknown  
41 and so far the only identified sensor for viral nucleic acids, a hallmark of viral infection, is  
42 the DEX/DH box helicase Dicer-2, which detects double stranded (ds) RNA and activates the  
43 RNAi pathway<sup>14</sup>. In mammals, STING binds a variety of cyclic dinucleotides (CDN)<sup>15,16</sup> but  
44 is most strongly activated by the second messenger 2'3'-cGAMP, which is produced by the  
45 enzyme cGAS<sup>2-5,17-20</sup>. We recently showed that injection of 2'3'-cGAMP into the body cavity  
46 of adult flies induces potent Sting signaling and triggers a broad antiviral protection,  
47 suggesting that pattern recognition receptors (PRRs) with CDN synthase activity sense viral  
48 infection in flies<sup>21</sup>.

49 The *D. melanogaster* gene *CG7194* was described as a homologue of cGAS<sup>22</sup>, but so far no  
50 enzymatic activity has been described and *CG7194* deficient flies appear to have a normal

51 antiviral immune response<sup>23</sup>. We identified four hitherto undescribed *D. melanogaster* gene  
52 products related to CG7194 and cGAS, of which two, CG12970 and CG30424, harbored a  
53 conserved active site compatible with CDN synthase activity (Fig. 1a). In the case of  
54 CG30424, the annotated start methionine is situated in the active site and would be  
55 incompatible with the fold of a CDN synthase. However, we identified an upstream in-frame  
56 start codon allowing for the translation of a functional CDN synthase (Extended Data Fig. 1).  
57 Interestingly, all candidates lack the characteristic Zn-finger motif as well as the secondary  
58 binding site found in cGAS, suggesting that their presumed interaction with nucleic acids  
59 must differ significantly (Extended Data Fig. 1). Thus, the *D. melanogaster* genome encodes  
60 two proteins with putative CDN synthase activity besides CG7194 and based on the data  
61 presented below, we named them cGAS-like receptor 1 and 2 (cGLR1 and cGLR2, encoded  
62 by *CG12970* and *CG30424*, respectively).

63 To test if the identified CDN synthases can activate signaling, we used the macrophage-like  
64 S2 cell line and a luciferase reporter system based on the promoter of the *Sting* gene since  
65 activation of *Sting* induces its own transcription<sup>11</sup>. Expression of human cGAS in S2 cells led  
66 to activation of the *Sting* reporter and this activation was abolished by mutation of the active  
67 site (Fig. 1b, Extended Data Fig. 2), agreeing with our previous discovery that transfection of  
68 2'3'-cGAMP in S2 cells triggers *Sting* signaling<sup>21</sup>. Expression of cGLR1 and cGLR2 resulted  
69 in significant upregulation of the *Sting* reporter, and mutation of their predicted active site  
70 abrogated this activity. Despite exhibiting the highest homology to human cGAS, CG7194  
71 did not yield any detectable activity in this assay. We conclude that we have identified two  
72 cGAS-like enzymes that could function as PRRs sensing viral infection in *D. melanogaster*.

73 To confirm these results *in vivo*, we generated transgenic flies expressing wild-type or  
74 catalytically inactive mutants of cGLR1 and cGLR2 using the heat-inducible Gal4-  
75 Gal80/UAS system<sup>24</sup>. We confirmed that both genes were overexpressed (Extended Data Fig.  
76 3a, b) at 29°C and that this did not have a major effect on the viability of the flies (Extended  
77 Data Fig. 3e). Expression levels of *Sting* and the *Sting*-regulated genes (*Srg*) 1, 2, and 3<sup>21</sup>  
78 were all significantly upregulated in flies overexpressing wild-type cGLR2 compared to the  
79 catalytically inactive mutant (Fig. 1c, d and Extended Data Fig. 3c, d). Similarly,  
80 overexpression of cGLR1 led to a significant upregulation of *Sting*, *Srg2*, and *Srg3*, whereas  
81 the trend observed for *Srg1* did not reach significance. Finally, overexpression of cGLR1 and  
82 cGLR2 led to a significant reduction of vesicular stomatitis virus (VSV) replication compared  
83 to the catalytically inactive mutants (Fig. 1e). Overexpression of cGLR2 also reduced

84 replication of *Drosophila* C virus (DCV), a natural *Drosophila* pathogen, whereas the slight  
85 reduction observed with cGLR1 was not significant for this virus (Fig. 1f). However,  
86 transgenic flies expressing the wild-type versions of cGLR1 and cGLR2, but not the  
87 catalytically inactive mutants, exhibited a striking increase in survival following infection  
88 with DCV (Fig. 1g). We conclude that cGLR1 and cGLR2 can initiate a transcriptional  
89 response *in vivo*, associated with protection against virus infection.

90 To test if signaling by cGLR1 and cGLR2 depends upon Sting, we introduced a frameshift  
91 deletion in the *Sting* gene of S2 cells (Extended Data Fig. 4d, e). Activation of the Sting  
92 reporter by cGLR1, cGLR2 and cGAS was abolished in the knockout cells but was rescued  
93 when co-transfecting with Sting (Extended Data Fig. 4a, b). Thus, Sting is required for  
94 cGLR1- and cGLR2-mediated signaling. Sting drives the expression of antiviral genes  
95 through Relish, a member of the NF- $\kappa$ B family of transcription factors<sup>11,21</sup>. Mutation of the  
96 Relish binding site within the *Sting* promoter abolished the response to cGLR1 and cGLR2,  
97 connecting these receptors to NF- $\kappa$ B-dependent transcription (Extended Data Fig. 4c). This is  
98 in contrast to the mammalian system, where members of the interferon regulatory factor  
99 (IRF) family of transcription factors mediate most of the antiviral effect<sup>25,26</sup>, whereas NF- $\kappa$ B  
100 is thought to primarily drive expression of pro-inflammatory cytokines.

101 To show that cGLR1 and cGLR2 are required for initiating an antiviral immune response in  
102 flies, we generated cGLR1 or cGLR2 knockout (KO) flies by CRISPR/Cas9 mutagenesis  
103 (Extended Data Fig. 5). Next, we generated cGLR1 and cGLR2 double KO flies by  
104 recombination (denoted cGLR1/2 KO). All flies were viable and resisted the stress of a buffer  
105 injection (Extended Data Fig. 6a). Upon infection with DCV cGLR1 KO but not cGLR2 KO  
106 flies exhibited reduced survival whereas the cGLR1/2 KO flies had a significantly lower  
107 survival than either of the two single KO flies (Fig. 2a). In agreement with the survival data,  
108 we observed a trend for increased DCV replication in cGLR1 KO flies compared to control  
109 and cGLR2 KO flies, which became statistically significant in the cGLR1/2 double KO flies  
110 (Fig. 2c). Finally, expression of Sting-regulated genes was reduced in both cGLR1 KO and  
111 cGLR1/2 KO flies (Fig. 2d and Extended Data Fig 6b, c, d). Next, we infected both cGLR1  
112 and cGLR2 KO flies with Kallithea virus (KV), a large DNA virus and also a natural  
113 *Drosophila* pathogen, and observed reduced survival in both KO flies (Fig. 2b and Extended  
114 Data Fig. 7a). However, this was not accompanied by a significant increase in viral  
115 replication in either KO flies (Fig. 2e). As previously reported<sup>27</sup>, KV did induce expression of  
116 Sting-regulated genes and this induction was lost in cGLR1 KO flies. Intriguingly, the

117 induction of *Srg3*, but not *Sting*, *Srg1*, and *Srg2*, was affected in cGLR2 KO flies (Fig. 2f and  
118 Extended Data Fig 7b, c, d). **Similar to what was observed for DCV, cGLR1/2 KO flies**  
119 **exhibited a more severe phenotype upon KV infection than single KO flies (Extended Data**  
120 **Fig. 7e, f, g).** We also tested infection by VSV and invertebrate iridescent virus 6 (IIV6), but  
121 neither of them showed any overt phenotype for survival and viral load (Extended Data Fig. 8  
122 and 9). However, we observed that one of the marker genes, *Srg3*, was induced by VSV and  
123 IIV6 infection in control and cGLR1 KO flies, but not in the cGLR2 KO flies (Extended Data  
124 Fig. 8g and 9g). We conclude that both cGLR1 and cGLR2 are required for survival of flies  
125 upon infection with two natural viral pathogens of *Drosophila*, DCV and KV.

126 Next, we expressed cGLR1, cGLR2 or cGAS alone or together with human STING in the  
127 human cell line HEK293T, which lacks endogenous expression of STING. Here, cGLR2  
128 induced signaling via STING to a level comparable to that of cGAS (Fig. 3a and Extended  
129 Data Fig. 10a). Furthermore, this depended upon the active site of cGLR2, suggesting that  
130 cGLR2 produces a CDN capable of activating STING (Extended Data Fig. 10b, c). In  
131 contrast, cGLR1 did not activate STING signaling in HEK293T cells, (Fig. 3a and Extended  
132 Data Fig. 10a). To identify the CDN synthesized by cGLR2, we isolated the nucleotide-  
133 containing fraction from HEK293T cells expressing cGLR2 and then subjected this extract to  
134 analysis by mass spectrometry. Interestingly, Slavik *et al.* demonstrate that cGLR1 produces  
135 3'2'-cGAMP<sup>28</sup>. We therefore established a protocol to detect both 2'3'-cGAMP and 3'2'-  
136 cGAMP, which revealed that the two CDNs are synthesized in approximately equivalent  
137 amounts by cGLR2 in HEK293T cells (Fig. 3b and Extended Data Fig. 10d, e, f). **Both 2'3'-**  
138 **cGAMP and 3'2'-cGAMP induced expression of *Sting* and *Srg3* when introduced into S2**  
139 **cells. The 2'3'-cGAMP mediated induction was lower than that of 3'2'-cGAMP but the**  
140 **difference was not statistically significant. The two CDNs also activated endogenous STING**  
141 **in the human cell line HT-1080, with 2'3'-cGAMP appearing the most potent activator**  
142 **(Extended Data Fig. 10g, h, i).** Therefore, we hypothesize that the absence of activity by  
143 cGLR1 in HEK293T cells is caused by the absence of a suitable activator. The cGLRs share  
144 similarity with oligoadenylate synthetases, a family of proteins activated by dsRNA, and thus  
145 we transfected HEK293T cells first with cGLR1 and then poly(I:C), which led to activation  
146 of cGLR1 (Fig. 3c). To confirm that cGLR1 is indeed activated by dsRNA, we expressed the  
147 protein in *E. coli*, purified it and then performed an *in vitro* activity assay as described by  
148 Kranzusch and colleagues<sup>28</sup>. This showed that cGLR1 produces 3'2'-cGAMP and minor  
149 amounts of 2'3'-c-diAMP upon stimulation with either poly(I:C) or a 100 base pair long

150 dsRNA produced by T7 transcription, but not with a similar 100 base pair long dsDNA (Fig.  
151 3d and Extended Data Fig. 11a, b). We also attempted to purify cGLR2 but only achieved  
152 poor quality protein preparations that did not display any activity.

153 Since cGLR2 is constitutively active when expressed in both HEK293T cell and S2 cells, we  
154 assume that these cells produce a suitable activator. When performing transfections, the  
155 transfected DNA can act as a ligand activating cGAS and potentially cGLR2. To circumvent  
156 this issue, we generated HEK293T cells stably expressing either cGAS or cGLR2 by  
157 retroviral transduction. cGAS only produced 2'3'-cGAMP upon transfection with DNA (Fig.  
158 3e). However, cGLR2 produced both 3'2'-cGAMP and 2'3'-cGAMP, regardless of the  
159 presence of cytosolic DNA supplied by transfection. Thus, we conclude that the ligand  
160 activating cGLR2 is not dsDNA. As demonstrated above, cGLR1 is inactive in HEK293T  
161 cells unless dsRNA is provided by transfection, indicating that dsRNA is not present in our  
162 HEK293T cells. Thus, the activity of cGLR2 in HEK293T cells cannot be explained by the  
163 presence of either dsRNA or dsDNA. It is possible that cGLR2 is constitutively active and to  
164 address this, we mutated residues in the putative nucleic acid-binding domain (K256E/R267E  
165 and K256E/R271E). Those residues are conserved in cGAS and oligoadenylate synthetases  
166 (OAS) and are known to be critical for DNA- and RNA-induced activation of these  
167 enzymes<sup>3,29</sup>. Mutation of those residues led to significant loss of activity in S2 cells and a  
168 complete loss of activity in HEK293T cells (Fig. 3f, Extended Data Fig. 11c, d). In summary,  
169 our data suggest that cGLR2 requires allosteric activation by a nucleic acid.

170 To conclude, we have identified two novel PRRs, cGLR1 and cGLR2, which orchestrate a  
171 Sting and NF- $\kappa$ B dependent antiviral immune response in *D. melanogaster*. Several  
172 primordial functions of Sting have been suggested, including sensing of bacteria through  
173 recognition of bacterially derived CDNs<sup>23</sup> or autophagy<sup>12,30</sup>. Our data suggest that a cGLR-  
174 Sting-NF- $\kappa$ B axis was present already during early metazoan evolution. They further reveal  
175 that the production of CDNs by metazoan enzymes is not limited to 2'3'-cGAMP. Different  
176 CDNs could lead to diverse signaling outcomes, interact with alternative receptors<sup>31</sup> or have  
177 different stability towards degradation by both host and viral encoded degrading enzymes,  
178 e.g. poxins<sup>32-34</sup>. Future studies are needed to determine the biological role of different  
179 cGAMP isomers.

180 The cGLRs are the first reported class of antiviral PRRs responsible for inducing a  
181 transcriptional response in insects. One striking difference between the cGLRs and cGAS is  
182 the specificity in activation. Whereas cGAS contains a Zn-finger motif inserted early in



183 vertebrate evolution, which confers specificity for DNA, the cGLRs have a nucleic acid-  
184 binding groove more akin to OAS. We show that cGLR1 is activated by dsRNA and this is  
185 consistent with our *in vivo* data, which reveal a strong susceptibility of cGLR1 mutant flies to  
186 DCV, a (+)ssRNA virus known to produce large amounts of long dsRNAs. Interestingly, our  
187 data suggest that cGLR2 is activated by a yet unidentified ligand. Both receptors may  
188 recognize different characteristics of the virally derived RNA, in a manner conceptually  
189 similar to the receptors RIG-I and MDA5 in mammals. In addition, we note that the  
190 expression of cGLR2 appears to be tightly regulated, with several splice isoforms  
191 differentially expressed (flybase.org/reports/FBgn0050424) and poor protein stability in S2  
192 but not HEK293T cells, suggesting alternative modes of regulation of this receptor.

193 We speculate that the cGLR class of PRRs is not only limited to cGAS, cGLR1, and cGLR2  
194 but might have expanded even further in metazoans. In particular, we cannot rule out that the  
195 previously identified cGAS candidate CG7194 is a third cGLR in *D. melanogaster* and that  
196 the missing activity is due to a lack of either the correct activator or a *bona fide* readout.  
197 Finally, the human genome harbors at least one uncharacterized gene, which shows similarity  
198 to cGAS and has a sequence compatible with a functional active site, making it a potential  
199 cGLR<sup>35</sup>.

200  
201 **Acknowledgements.** The authors wish to thank Kailey Slavik and Philip Kranzusch for  
202 discussing and sharing information prior to publication, Peter E. Andersen for help with  
203 generating Sting knockout S2 cells, Darren Obbard for providing Kallithea virus and C.  
204 Meignin, J. Marques, J. Schneider and G. Haas for helpful discussions. R.H was supported by  
205 grants from the Novo Nordisk Foundation (NNF17OC0028184) and the Danish Council for  
206 Independent Research (4183-0032B and 0135-00338B). J.L.I. was supported by Agence  
207 Nationale de la Recherche (ANR-17-CE15-0014), Investissement d'Avenir Programs (ANR-  
208 10-LABX-0036, ANR-11-EQPX-0022), Institut Universitaire de France and the Chinese  
209 National Overseas Expertise Introduction Center for Discipline Innovation (Project "111"  
210 (D18010)). H.C was supported by the Natural Science Foundation (32000662) and the  
211 Foreign Experts Program (2020A1414010306). A.P. was supported by an ERC consolidator  
212 grant (ERC-CoG ProDAP, 817798) and grants from the German Research Foundation (PI  
213 1084/5, TRR179, and TRR237).

214 **Author contributions.** A.H., K.G.W., H.H.G., H.C., J.L.I., and R.H. conceived and designed  
215 experiments for this study. A.H., K.G.W., H.H.G., X.A., Y.C., L.L., Z.W., H.D., J.L., N.A.F.,  
216 B.S., L.L.A., K.K., L.D. and H.C. performed experiments. A.H., H.H.G., and H.C. created  
217 the figures. H.C., A.P., J.L.I., and R.H. supervised the study. A.H., J.L.I. and R.H. wrote the  
218 original draft of the manuscript and all authors participated in reviewing and editing it.

219 **Competing interests.** The authors declare that they have no competing interests.

220

## 221 **Methods**

### 222 **Alignment of cGAS-like proteins**

223 The five cGAS-like candidate proteins from *D. melanogaster*, CG12970 (UniProt: A1ZA55),  
224 CG30424 (UniProt: A8DYP7), CG4746 (UniProt: Q9U3W6), CG4766 (UniProt: Q9Y106),  
225 and CG7194 (UniProt: Q9VSH0) were aligned with porcine OAS1 (UniProt: Q29599),  
226 human OAS1 (UniProt: P00973-1), human cGAS (UniProt: Q8N884-1), porcine cGAS  
227 (UniProt: I3LM39), murine cGAS (UniProt: Q8BSY1) using CLC Main Workbench 7.7.2  
228 (QIAGEN). Structurally homologous secondary structure elements of the mammalian  
229 nucleotidyltransferases were used as alignment fix points.

230

### 231 **Cell lines**

232 HEK293T and HT-1080 cells were obtained from ATCC (CRL3216) and the German  
233 Collection of Microorganisms and Cell Cultures (ACC 315), respectively, whereas  
234 HEK293T/MAVS KO cells were a kind gift from Veit Hornung (Gene Center Munich). All  
235 mammalian cells were cultured in Dulbecco's modified Eagle medium (DMEM) (Sigma-  
236 Aldrich) supplemented with 10% fetal bovine serum (FBS) (Biowest), 100 U ml<sup>-1</sup> penicillin  
237 (Sigma-Aldrich) and 100 µg ml<sup>-1</sup> streptomycin (Sigma-Aldrich) at 37° C and 5% CO<sub>2</sub>.  
238 Schneider 2 (S2) cells were obtained from the German Collection of Microorganisms and  
239 Cell Cultures (ACC 130) and cultured in Schneider's Drosophila Medium (Biowest)  
240 supplemented with 10% FBS, 100 U ml<sup>-1</sup> penicillin (Sigma-Aldrich) and 100 µg ml<sup>-1</sup>  
241 streptomycin (Sigma-Aldrich) at 27 °C.

242

### 243 **Fly lines**

244 Fly stocks were raised on standard cornmeal agar medium at 25°C. All fly lines used in this  
245 study were free of Wolbachia. The drivers used were [*actin5C-Gal4/CyO*; *tubulin-*



246 Gal80<sup>ts</sup>/TM6,Tb]. Transgenic lines for expression of GFP and  $\beta$ -galactosidase (P{UAS-  
247 GFP.nls}8 line (BDSC #4776) and P{UAS-LacZ.Exel}2 (BDSC #8529)) were obtained from  
248 the Bloomington Drosophila Stock Center. For the UAS transgenic lines of wild-type and  
249 AFA mutant versions of cGLR1 and cGLR2, the corresponding versions of the cDNAs (RD  
250 isoform in the case of cGLR2) were cloned into pUAST-attB vectors. The resulting plasmids  
251 were injected into embryos of [*y*<sup>l</sup> *M{vas-int.Dm}ZH-2A w\**; *M{3xP3-RFP-attP}ZH-86Fb*]  
252 flies (BDSC #24749). Individual males from the injected embryos were then crossed with  
253 flies containing the third chromosome balancers *TM6B,Tb/TM3,Sb* to establish balanced  
254 stocks. *cGLR1* and *cGLR2* knockout flies were generated by CRISPR-Cas mediated  
255 mutagenesis. Briefly, sgRNA encoding pUAST-attB plasmids were injected into embryos of  
256 *y*<sup>l</sup> *M{vas-int.Dm}ZH-2A w\**; *M{3xP3-RFP.attP}ZH-86Fb* (BDSC#24749) flies. The resulting  
257 transgenic flies were then crossed with *y*<sup>l</sup> *w*<sup>1118</sup>; *attP2{nos-Cas9}/TM6C, Sb Tb [y+]* flies  
258 obtained from the National Institute of Genetics. Individual males from the F1 were then  
259 crossed with *yw; Bc,Gla/CyO* flies to establish stocks from the *CyO* progeny. This progeny  
260 was then scored for mutations by Sanger sequencing (Guangzhou IGE Biotechnology).  
261 *cGLR1* (2R: 52C8) and *cGLR2* (2R: 60E11) knockout flies were isogenized to the DrosDel  
262 *w*<sup>1118</sup> isogenic background to reduce the genetic background effects. For each line, the non-  
263 mutated chromosomes were replaced using balancer chromosomes (*w*<sup>1118</sup>; *If/CyO; TM3/TM6*  
264 and *w*<sup>1118</sup>; *If/CyO*) whereas the mutations were recombined to the respective DrosDel *w*<sup>1118</sup>  
265 isogenic chromosome for seven generations. We confirmed that the isogenized lines retained  
266 the mutation of interest by DNA sequencing. *cGLR1* and *cGLR2* double knockout flies were  
267 generated by crossing the two single knockout flies. Females from the progeny were crossed  
268 with *w*<sup>1118</sup>; *If/CyO* to establish the stocks from the *CyO* progeny. Presence of the double  
269 mutation upon recombination on the right arm of the second chromosome in this progeny was  
270 established by DNA sequencing. All the crossing schemes and detailed injection protocols  
271 are available upon request.

272

## 273 **Plasmids**

274 cDNAs encoding human cGAS (amino acids 155-522), cGLR1, cGLR2 or CG7194 with a C-  
275 terminal V5- or triple FLAG-tags were cloned into the pAc5.1 vector for transient expression  
276 in S2 cells, the pcDNA3.1 vector for transient expression in HEK293T cells or the pCCL-  
277 PGK vector for production of lentiviral particles. For expression of cGLR1 in *E. coli*, the  
278 cDNA was cloned into the pET-9d vector in between an N-terminal TEV protease cleavage

279 site and maltose-binding protein (MBP) and a C-terminal polyhistidine-tag. The following  
280 active site mutants were generated by site-directed mutagenesis: cGAS AFA (E225A  
281 D227A), cGLR1 AFA (E71A D73A), cGLR2 AFA (E79A D81A), and CG7194 AFA (E70A  
282 D72A). cDNAs encoding human or *D. melanogaster* STING/Sting without or with a C-  
283 terminal V5-tag were cloned into the pcDNA3.1 and pAc5.1 vector, respectively. Plasmids  
284 expressing firefly luciferase under transcriptional control of the proximal 200 base pairs of  
285 the *D. melanogaster* *Sting* promoter or a mutated version of the promoter containing two  
286 point mutations in the Relish binding site have previously been described and so has the  
287 plasmid constitutively expressing *Renilla* luciferase in S2 cells<sup>11</sup>. Plasmids expressing firefly  
288 luciferase under transcriptional control of the proximal 200 base pairs of the human *IFNBI*  
289 promoter or constitutively expressing *Renilla* luciferase in HEK293T cells have also been  
290 previously described<sup>36</sup>.

291

### 292 **Transfection of S2 cells**

293 To test induction of *D. melanogaster* *Sting* by cGLRs, 12-well tissue culture plates were  
294 seeded with  $6 \times 10^5$  S2 cells per well. After 24 h, each well was transfected with 485 ng  
295 pGL3 plasmid expressing firefly luciferase under transcriptional control of the *Sting*  
296 promoter, 15 ng pAc5.1 plasmid constitutively expressing *Renilla* luciferase, 400 ng pAc5.1  
297 plasmid expressing cGAS, cGLR1, cGLR2 or CG7194 or their corresponding mutants  
298 (except Extended Data Fig. 10b where 10 ng was used) and finally empty Ac5.1 plasmid to  
299 reach a total amount of 1  $\mu$ g plasmid per well. To test if the activity of cGLRs is *Sting*-  
300 dependent, 12-well tissue culture plates were seeded with  $6 \times 10^5$  S2 or *Sting* knockout S2  
301 cells per well. After 24 h, each well was transfected with 485 ng pGL3 plasmid expressing  
302 firefly luciferase under transcriptional control of the *Sting* promoter, 15 ng pAc5.1 plasmid  
303 constitutively expressing *Renilla* luciferase, 30 ng pAc5.1 plasmid expressing *Sting*, 100 ng  
304 pAc5.1 plasmid expressing cGAS, cGLR1, cGLR2 or CG7194 and finally Ac5.1 plasmid to  
305 reach a total amount of 1  $\mu$ g plasmid per well. All transfections of S2 cells were performed  
306 using jetOPTIMUS (Polyplus Transfection) according to the manufacturer's instructions.

307

### 308 **Transfections of HEK293T cells**

309 To test induction of human STING by cGLRs, 12-well tissue culture plates were seeded with  
310  $3 \times 10^5$  HEK293T cells per well. After 24 h, each well was transfected with 970 ng pGL3  
311 plasmid expressing firefly luciferase under transcriptional control of the *IFNBI* promoter, 30  
312 ng pRL plasmid constitutively expressing *Renilla* luciferase, 100 ng pcDNA3.1 plasmid

313 expressing STING, 400 ng pcDNA3.1 plasmid expressing cGAS, cGLR1, cGLR2 or CG7194  
314 and finally empty pcDNA3.1 plasmid to reach a total amount of 2 µg plasmid per well. For  
315 each well, the DNA was dissolved in 100 µl DMEM and likewise 6 µg polyethylenimine  
316 (PEI)(Polysciences) was dissolved in 100 µl DMEM. The DNA and PEI was then mixed and  
317 incubated for 20 min before adding it dropwise to the cells.

318 To test activation of cGLR1 by poly(I:C), 48-well tissue culture plates were seeded with 9 x  
319 10<sup>4</sup> HEK293T/MAVS KO cells per well. After 24 h, each well was transfected with 242.5 ng  
320 pGL3 plasmid expressing firefly luciferase under transcriptional control of the *IFNBI*  
321 promoter, 7.5 ng pRL plasmid constitutively expressing *Renilla* luciferase, 10 ng pcDNA3.1  
322 plasmid expressing STING, 240 ng pcDNA3.1 plasmid expressing cGLR1 and finally empty  
323 pcDNA3.1 plasmid to reach a total amount of 500 ng plasmid per well. After another 3 h,  
324 cells were transfected 150 ng Vaccigrade™ Poly(I:C)(InvivoGen) per well. Both kind of  
325 transfection were done using Lipofectamine 2000 (Fisher Scientific) following to the  
326 manufacturer's instructions.

327 To test production of CDNs by cGLR2 via mass spectrometry, HEK293T cells were grown in  
328 T175 tissue culture flasks and transfected at a confluence of 60-70%. For each flask 87.5 µg  
329 pcDNA3.1 plasmid expressing EGFP, cGAS or cGLR2 was dissolved in 4.4 ml DMEM and  
330 262.5 µg PEI were dissolved in 4.4 ml DMEM. The DNA and PEI was then mixed and  
331 incubated for 20 min before added to the cells.

332

### 333 **Transduction of HEK293T cells**

334 Lentiviral particles were made as previously described<sup>37</sup>. For transduction of HEK293T cells,  
335 the cells were grown in T75 tissue culture flasks and transduced at a confluence of 60-70%  
336 with filtered supernatants. The cells were then passaged for 1 week before being subjected to  
337 further experiments. Transfection of transduced cells was performed using pcDNA3.1  
338 plasmid expressing EGFP as described above.

339

### 340 **Measuring luciferase activity of transfected cells**

341 Cells were lysed in 200 µl Passive Lysis Buffer (Promega) per well and afterwards the lysates  
342 were centrifuged at 14,000g for 5 min to remove cell debris. Firefly and *Renilla* luciferase  
343 activity was measured on 10 µl lysate using the Dual-Luciferase® Reporter Assay System  
344 (Promega).

345

### 346 **Immunoblotting**

347 Cell lysates were subjected to SDS-PAGE and proteins were transferred to a polyvinylidene  
348 fluoride membrane. Blotted proteins were detected with Anti-V5 Antibody  
349 (Invitrogen)(diluted 1:5,000), Anti-Actin, clone 4 (EMD Millipore)(diluted 1:5,000), Anti-  
350 Sting (BioGenes)(1:500), Monoclonal ANTI-FLAG® M2 (Sigma-Aldrich)(diluted 1:2,000)  
351 or STING (D2P2F) Rabbit mAb (Cell Signaling Technology)(diluted 1:1,000) primary  
352 antibody and a Peroxidase-conjugated AffiniPure F(ab')<sub>2</sub> Fragment Donkey Anti-Mouse IgG  
353 (JacksonImmunoResearch)(diluted 1:15,000) or Anti-Rabbit IgG, HRP-linked Antibody (Cell  
354 Signalling Technology)(diluted 1:3,000) secondary antibody. Blots were developed with  
355 SuperSignal™ West Dura Extended Duration Substrate. The Anti-Sting antibody was raised  
356 in rabbit against the peptide HMQNKTKTIDEISN. The antibody was affinity purified from  
357 serum using the peptide and verified by immunoblotting of recombinant Sting made in  
358 *Escherichia coli*.

359

### 360 **Generation of Sting knockout cells by CRISPR-Cas9**

361 Three CRISPR RNAs targeting the first translated exon in the *D. melanogaster* *Sting* gene  
362 were cloned into the pAc-sgRNA-Casp vector. After transfection, S2 cells were grown under  
363 selection with 5 µg ml<sup>-1</sup> puromycin for two weeks. Individual clones were isolated by  
364 limiting dilution and then screened for a non-functional Sting pathway. Knockout of Sting  
365 was verified by immunoblotting and Sanger sequencing.

366

### 367 **Mass spectrometry**

368 Transfected HEK293T cells were washed with PBS, trypsinized and resuspended in DMEM  
369 before being harvested by centrifugation at 800g for 5 min. The medium was carefully  
370 removed and the cells resuspended in PBS before being collected by centrifugation at 800g  
371 for 5 min. After another final washing step, the cells were lysed with 500 µL 60% MeOH and  
372 vortexed for 15 seconds. For the spike in samples, 20 nmol of either 2'3'-cGAMP  
373 (Invivogen) or 3'2'-cGAMP (BioLog) were added to lysates from GFP transfected cells. The  
374 lysates were frozen in liquid nitrogen and stored at -80°C for further analysis. 20 nmol ATP-  
375 γ-S (Jena Bioscience NU-506-5) were added to all lysates and nucleotides were purified from  
376 the lysates as previously described<sup>38</sup> and then analyzed by means of LC-MS/MS with a 5500  
377 QTrap (AB Sciex, Darmstadt, Germany) and a ExionLC AD UPLC (AB Sciex). For  
378 chromatographic separation, a Xbridge Amid 3.5 µm, 150 x 2.1 mm column (Waters) was  
379 used with acetonitrile/water with 5 mM ammonium acetate (50/50, v/v, pH 9.5) as solvent A  
380 and acetonitrile/water with 5 mM ammonium acetate (95/5, v/v, pH 9.5) as solvent B. A

381 linear gradient from 97% B to 50% B in 16 min was used. Afterward the column was flushed  
382 and equilibrated to starting conditions. The separation of 2'3'-cGAMP, 3'2'-cGAMP and  
383 ATP- $\gamma$ -S was performed using a 400  $\mu\text{L min}^{-1}$  flowrate at 40°C column oven temperature.  
384 Ions were analyzed by mass spectrometry in the negative ionization mode. The spray voltage  
385 was set to -4,500 V at a source temperature of 450°C using nitrogen as collision gas. The  
386 parameters for the collision-activated dissociation (CAD) were: medium, curtain gas: 35 psi,  
387 ion source gas 1: 55 psi, ion source gas 2: 65 psi, entrance potential (EP) -10 V and the dwell  
388 time 150 msec. The MRM (multiple reaction monitoring) transition for each compound were  
389 as follow: cGAMP: 672.987  $\rightarrow$  79.1 (quantifier), declustering potential (DP) -205 V,  
390 collision energy (CE) -160 V, Cell Exit Potential (CXP) -5 V; 672.987  $\rightarrow$  150.0 (qualifier),  
391 DP -205V, CE -52 V, CXP -7 V; ATP- $\gamma$ -S: 521.70  $\rightarrow$  78.8 (quantifier), DP -115 V, CE -128  
392 V, CXP -11 V; 521.70  $\rightarrow$  426.0 (qualifier), DP -115 V, CE -32 V, CXP -17 V. Analyst 1.7.  
393 was used to acquire the data and MultiQuant 3.0.3 was used to analyze the data (both AB  
394 Sciex).

395

### 396 **Expression and purification of recombinant protein**

397 *E. coli* BL21 (DE3) cells transformed with a pET-9d plasmid encoding cGLR1 were grown at  
398 37 °C in lysogenic broth medium containing 30  $\mu\text{g/ml}$  kanamycin until the culture reached an  
399  $\text{OD}_{600}$  of 0.4–0.5. Protein expression was then induced with 1 mM isopropyl-b-d-  
400 thiogalactopyranoside and the cells were incubated for another 12 h at 16 °C. Afterwards, the  
401 cells were harvested by centrifugation, resuspended in Lysis Buffer (50 mM  $\text{NaH}_2\text{PO}_4$ ,  
402 500 mM NaCl, 10% glycerol, 5 mM  $\beta$ -mercaptoethanol, 1 mM PMSF, 200  $\mu\text{g ml}^{-1}$  lysozyme,  
403 pH 7.4) and lysed by sonication. Following lysis, cell debris was removed by centrifugation  
404 at 18,500 ref for 60 min after which the supernatant was incubated with HisPur Ni-NTA  
405 Resin (ThermoFisher Scientific) at 4 °C for 1 h while continuously shaking. The resin was  
406 then transferred to a gravity flow column and washed with 20 column volumes (CV) of Wash  
407 Buffer (50 mM  $\text{NaH}_2\text{PO}_4$ , 200 mM NaCl, 2 M urea, 10% glycerol, 5 mM  $\beta$ -mercaptoethanol,  
408 pH 7.4) before eluting the protein with 5 CV of Elution Buffer (25 mM HEPES, 500 mM  
409 NaCl, 500 mM imidazole, 10% glycerol, 5 mM  $\beta$ -mercaptoethanol, pH 7.4). ). The eluate  
410 was diluted 2.5 times with Dilution Buffer (25 mM HEPES, 200 mM KCl, 5% glycerol, 5  
411 mM dithiothreitol (DTT), pH 7.4) and then applied to a MBPTrap 1 ml column (Cytiva).  
412 Bound protein was eluted with 5 CV Elution Buffer (20 mM HEPES, 200 mM KCl, 10%  
413 glycerol, 10 mM maltose, pH 7.4) and TEV protease (one twentieth of the total protein  
414 concentration) was added before dialysis overnight at 4°C against Dialysis Buffer (25 mM

415 Tris, 200 mM KCl, 5% glycerol, 5 mM DTT, pH 7.4). Finally, the protein was aliquoted and  
416 flash frozen in liquid nitrogen before being stored at  $-80^{\circ}\text{C}$ .

417

### 418 ***In vitro* activity assay**

419 cGLR1 activity was measured in a 50  $\mu\text{l}$  reaction volume containing 100  $\mu\text{g}/\text{ml}$  recombinant  
420 cGLR1, 240  $\mu\text{M}$  ATP, 240  $\mu\text{M}$  GTP, 1 mM  $\text{MnCl}_2$ , 1 mM  $\text{MgCl}_2$ , 120 mM KCl and 2.5  $\mu\text{g}$   
421 poly(I:C) (GE Healthcare), dsRNA (100 bp) or dsDNA (100 bp). The dsRNA was made as  
422 previously described<sup>39</sup> whereas the dsDNA was made by purchasing complementary sense  
423 and antisense ssDNAs (Sigma-Aldrich) with sequences corresponding to the dsRNA and then  
424 annealing them. The reactions were incubated at  $27^{\circ}\text{C}$  for 4 h and then terminated at  $95^{\circ}\text{C}$  for  
425 15 min. To digest non-cyclic nucleotides, the reactions were afterwards incubated with 10 U  
426 alkaline phosphatase (Roche) at  $37^{\circ}\text{C}$  overnight and again terminated at  $95^{\circ}\text{C}$  for 15 min. The  
427 terminated reactions were applied to anion exchange chromatography as previously  
428 described<sup>40</sup> and 3',2'-cGAMP was quantified by integrating the corresponding peaks on the  
429 chromatogram using the software Unicorn 5.10 (GE Healthcare) with default settings.

430

### 431 **Treatment with CDNs**

432 12-well tissue culture plates were seeded with  $3 \times 10^5$  HT-1080 or  $3 \times 10^6$  S2 cells per well.  
433 After 20 h, the medium was removed and 800  $\mu\text{l}$  digitonin buffer (100 mM KCl, 85 mM  
434 sucrose, 50 mM HEPES, 3 mM  $\text{MgCl}_2$ , 1 mM ATP, 0.1 mM GTP, 0.1 mM DTT, 0.2 %  
435 bovine serum albumin, pH 7.0) with or without 5  $\mu\text{M}$  2',3'-cGAMP or 3',2'-cGAMP (Biolog  
436 Life Science Institute) was added to the wells. The cells were incubated for 10 min before the  
437 digitonin buffer was removed and replaced with normal medium.

438

### 439 **Ectopic expression of cGLRs in transgenic flies**

440 cGLRs were expressed in transgenic flies using the heat-controlled Gal4/Gal80 system.  
441 Briefly, the UAS-Gal4>cGLR transgenic flies were crossed with the driver line [*actin5C*-  
442 Gal4/CyO; *tubulin*-Gal80<sup>ts</sup>/TM6,Tb] at  $25^{\circ}\text{C}$ . Males from F1 were collected and shifted to  
443  $29^{\circ}\text{C}$  for 5 days to block the repressive function of Gal80 to Gal4 and drive the expression of  
444 the transgenes.

445

### 446 **Viral infections**

447 Viral stocks were prepared in 10 mM Tris-HCl, pH 7.5. Infections were performed with adult  
448 flies by intrathoracic injection (Nanoject II apparatus, Drummond Scientific) with 4.6 nL of



449 DCV (5 (survival) or 500 (gene induction and viral load) PFU/fly), KV (10,000 ID<sup>50</sup>/fly),  
450 VSV (5,000 PFU/fly) or IIV6 (5,000 PFU/fly) viral suspension.

451

### 452 **RNA extraction from cells and flies and quantification of gene expression by qPCR**

453 RNA was extracted, cDNA was synthesized, and gene expression was quantified by qPCR as  
454 previously described<sup>21,37</sup>. Gene expression was analysed using the CFX Maestro Software  
455 (Bio-Rad).

456

### 457 **Statistical analyses**

458 All statistical analyses were done using GraphPad Prism 9.0.1 (GraphPad Software).  
459 Comparisons between groups were analysed using two-way ANOVA and Holm Holm-Šidák  
460 post hoc test, except for comparison of viral RNA load and survival of flies. For comparison  
461 of viral load, data were log transformed and then analyzed using one-way ANOVA and  
462 Dunnett T3 post hoc test whereas survival of flies was compared using log-rank test. Sample  
463 sizes (n) for each experiment are stated in the figure legends.

464

### 465 **Data Availability Statement**

466 The authors declare that the data supporting the findings of this study are available within the  
467 paper. The sequences and structures used in this study are CG12970 (UniProt: A1ZA55),  
468 CG30424 (UniProt: A8DYP7), CG4746 (UniProt: Q9U3W6), CG4766 (UniProt: Q9Y106),  
469 CG7194 (UniProt: Q9VSH0), porcine OAS1 (UniProt: Q29599), human OAS1 (UniProt:  
470 P00973-1), human cGAS (UniProt: Q8N884-1), porcine cGAS (UniProt: I3LM39), murine  
471 cGAS (UniProt: Q8BSY1), and murine cGAS in complex with DNA and a cGAMP  
472 intermediate analog (PDB: 4K98).

473

474

475

476

477

478

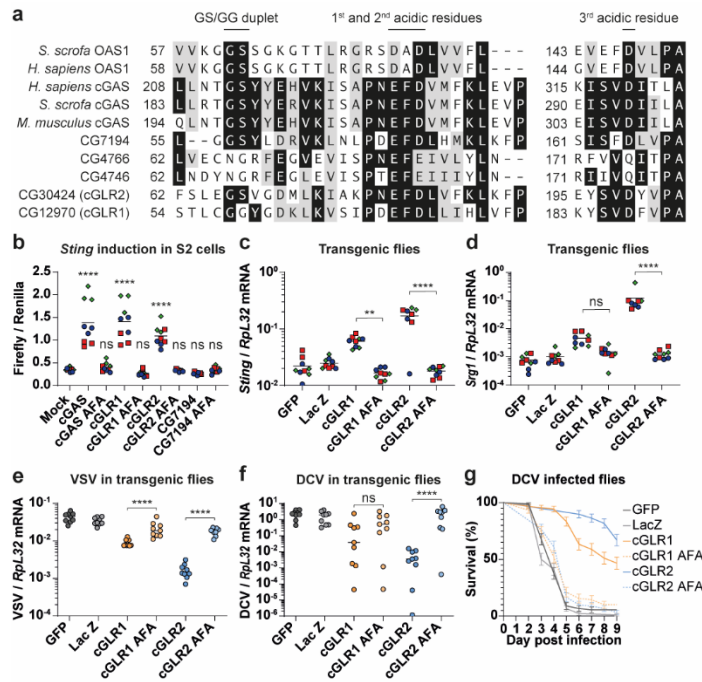
479

480

481

482

483  
484  
485  
486  
487  
488  
489  
490  
491  
492  
493  
494  
495  
496  
497  
498  
499  
500  
501  
502  
503  
504



505

506

507

508

509

510

511

512

513

514

515

516

517

518

519

520

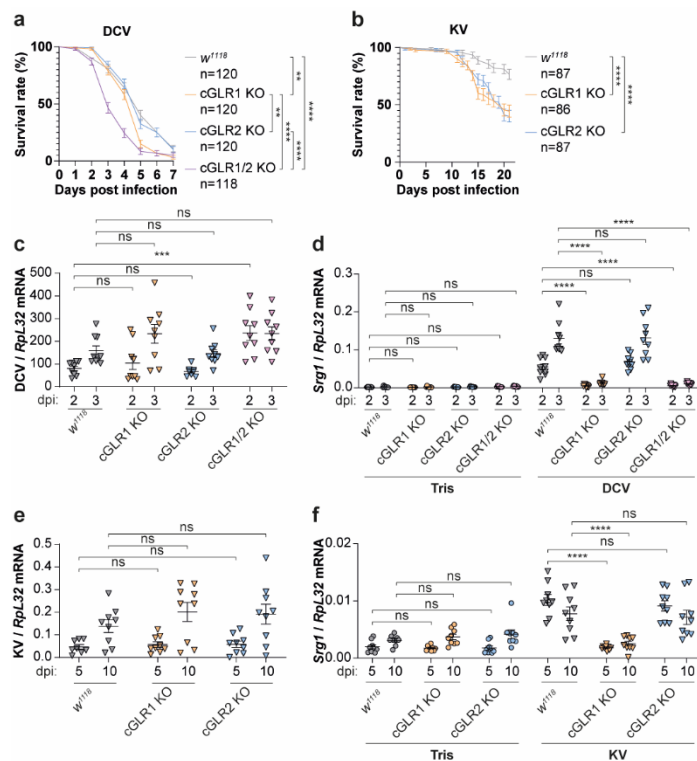
521

522

523

524

**Fig. 1 | cGRL1 and cGRL2 activate the Sting pathway and protect against viral infection.** **a**, Truncated alignment of identified cGAS-like candidates, mammalian cGAS and the structurally related OAS1. Essential active site residues (the GS/GG duplet and the metal ion coordinating acidic residues) are indicated above the alignment. **b**, *Sting* reporter activity in S2 cells transfected with cGAS-like candidates or their corresponding active site mutants (AFA). **c**, **d**, Expression of *Sting* (**c**) and *Srgl* (**d**) was monitored by RT-qPCR in transgenic flies ectopically expressing wild-type or mutant cGRLs. In **b**, **c**, **d**, data are from three independent experiments (blue, red, and green, each performed in triplicate) and shown with mean ( $n = 9$ ). **e**, **f**, VSV (**e**) or DCV (**f**) viral RNA load measured at 4 or 3 days, respectively, post infection in transgenic flies ectopically expressing wild-type or mutant cGRLs. Data are from three independent experiments, each performed in triplicates, and shown with mean ( $n = 9$ ). **g**, Flies expressing the indicated transgenes were injected with DCV and survival was monitored daily. Data are from 3 independent experiments, each with 30 flies ( $n = 90$ ). In **b**, **c**, and **d**, data were analyzed using two-way ANOVA and Holm-Šidák post hoc test and compared to mock (**a**) or relevant AFA mutants (**b**, **c**, **d**). In **e**, and **f**, Log transformed data were analyzed using one-way ANOVA and Dunnett T3 post hoc test and compared to relevant AFA mutants. In **g**, log-rank test was used to compare cGRL1 vs. cGRL1 AFA ( $P < 0.0001$ ) and cGRL2 vs. cGRL2 AFA ( $P < 0.0001$ ). ns not significant, \*\*  $P < 0.01$ , \*\*\*\*  $P < 0.0001$ .



525

526

527

528

529

530

531

532

533

534

535

536

537

538

539

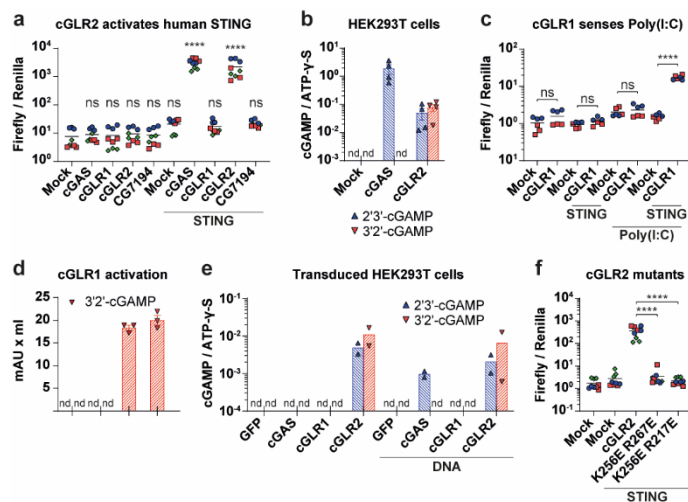
540

541

542

543

**Fig. 2 | Loss of cGLR1 or cGLR2 leads to an impaired antiviral immune response *in vivo*.** **a, b,**  $w^{1118}$ , cGLR1 KO, cGLR2 KO or cGLR1/2 KO flies were injected with DCV and survival was monitored daily. Data are from four independent experiments, each with three independent groups of around 10 flies. **b,**  $w^{1118}$ , cGLR1 KO or cGLR2 KO flies were injected with KV and survival was monitored daily. Data are from three independent experiments, each with three independent groups of around 10 flies. **c, d,**  $w^{1118}$ , cGLR1 KO, cGLR2 KO or cGLR1/2 KO flies were injected with DCV or Tris and viral load (**c**) as well as expression of *Srg1* (**d**) were monitored by RT-qPCR at 2 and 3 days post-injection (dpi). **e, f,**  $w^{1118}$ , cGLR1 KO or cGLR2 KO flies were injected with KV or Tris and viral load (**e**) as well as expression of *Srg1* (**f**) were monitored by RT-qPCR at 5 and 10 days post-infection (dpi). For panels c-f, expression was normalized to the housekeeping gene *RpL32* and data are from three independent experiments, each performed in triplicates ( $n = 9$ ). In **a** and **b**, log-rank test was used to compare the survival curves pairwise followed by a Holm-Šídák multiple comparison correction. In **c** and **e**, Log transformed data were analyzed using one-way ANOVA and Dunnett T3 post hoc test and compared to  $w^{1118}$  flies. In **d** and **f**, data were analyzed using two-way ANOVA and Holm-Šídák post hoc test and compared to  $w^{1118}$  flies. ns not significant, \*\*  $P < 0.01$ . \*\*\*  $P < 0.001$ . \*\*\*\*  $P < 0.0001$ .



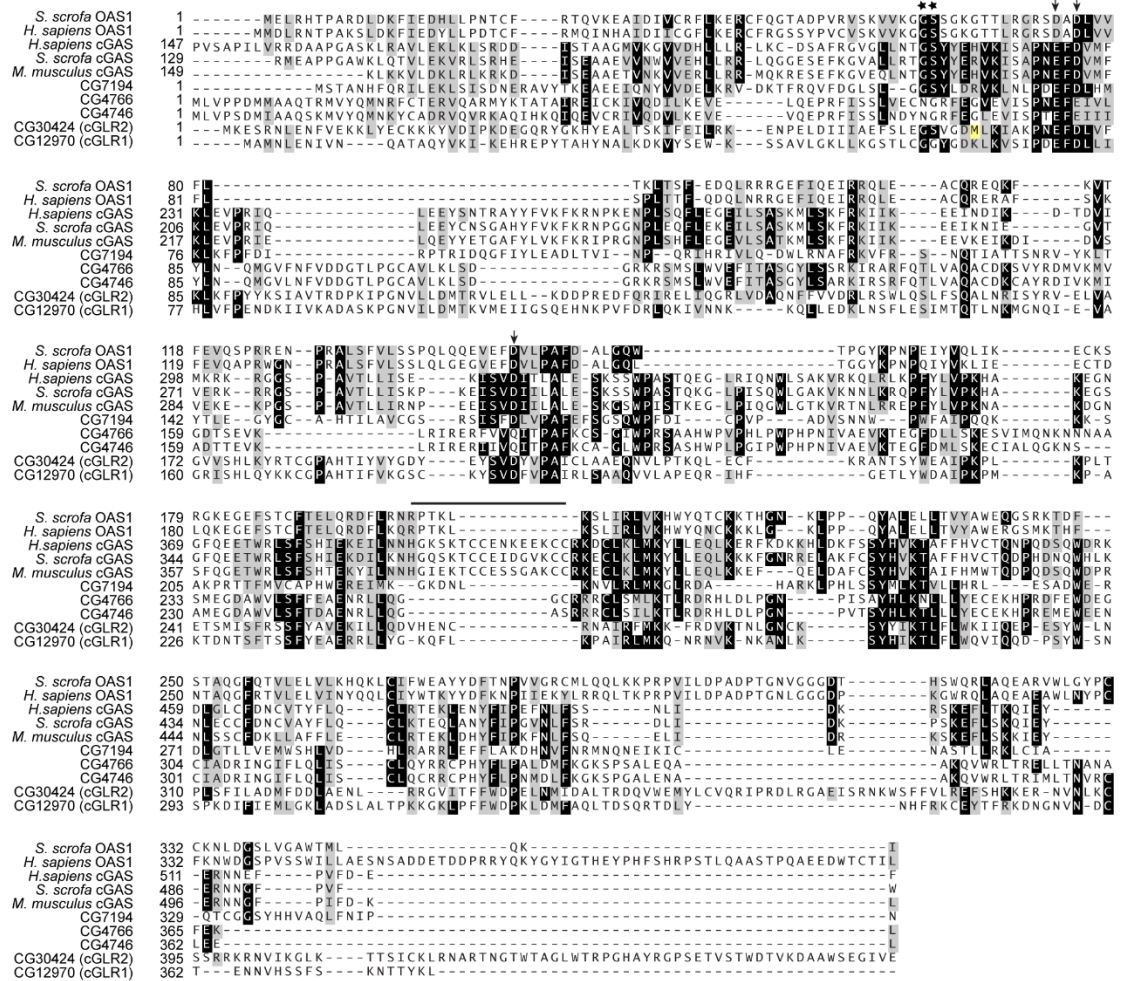
544

545 **Fig. 3 | cGRL1 is activated by dsRNA whereas cGRL2 is activated by an unidentified**  
 546 **molecule. a**, *IFNβ1* reporter activity in HEK293T cells transfected with cGAS-like  
 547 candidates and human STING. Data are from three independent experiments (blue, red, and  
 548 green, each performed in triplicates) and are shown with mean (n = 9). **b**, Quantification by  
 549 mass spectrometry of 2'3'-cGAMP or 3'2'-cGAMP production by HEK293T cells  
 550 transfected with GFP, cGAS or cGRL2. Data are from four independent experiments and  
 551 shown as mean ± s.e.m. (n = 4). **c**, *IFNβ1* reporter activity in HEK293T/MAVS KO cells  
 552 transfected first with cGRL1 and human STING and afterwards with poly(I:C). Data are from  
 553 two independent experiments (blue and red, each performed in triplicates) and are shown  
 554 with mean (n = 9). **d**, Quantification by anion exchange chromatography analysis of 3'2'-  
 555 cGAMP production by recombinant cGRL1 in the presence of different nucleic acids. Data  
 556 are from three independent experiments and shown as mean ± s.e.m. (n = 3). **e**, Quantification  
 557 by mass spectrometry of 2'3'-cGAMP or 3'2'-cGAMP production by HEK293T cells  
 558 transduced with GFP, cGAS, cGRL1 or cGRL2 and subsequently transfected with DNA.  
 559 Data are from two independent experiments (n = 2). **f**, *IFNβ1* reporter activity in HEK293T  
 560 cells transfected with wild-type cGRL2 or the indicated mutants and human STING. Data are  
 561 from three independent experiments (blue, red, and green, each performed in triplicates) and  
 562 are shown with mean (n = 9). In **a**, **c** and **f**, data were analyzed using two-way ANOVA and  
 563 Holm-Šidák post hoc test and compared to mock (**a**) or as indicated (**c**, **f**). nd not detected; ns  
 564 not significant, \*\*\*\*  $P < 0.0001$ .

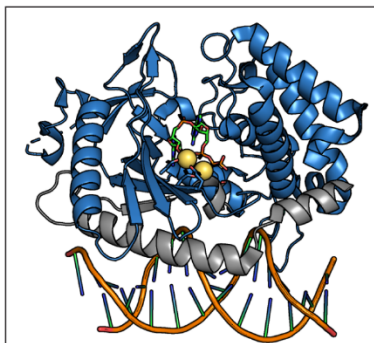
565

Extended Data Fig. 1 | Alignment of mammalian cGAS/OAS1 proteins and cGAS-like proteins from *D. melanogaster*

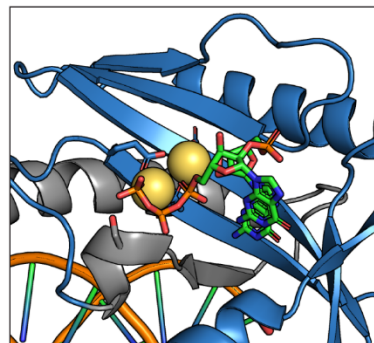
a



b



c



566

567

568

569

570

571

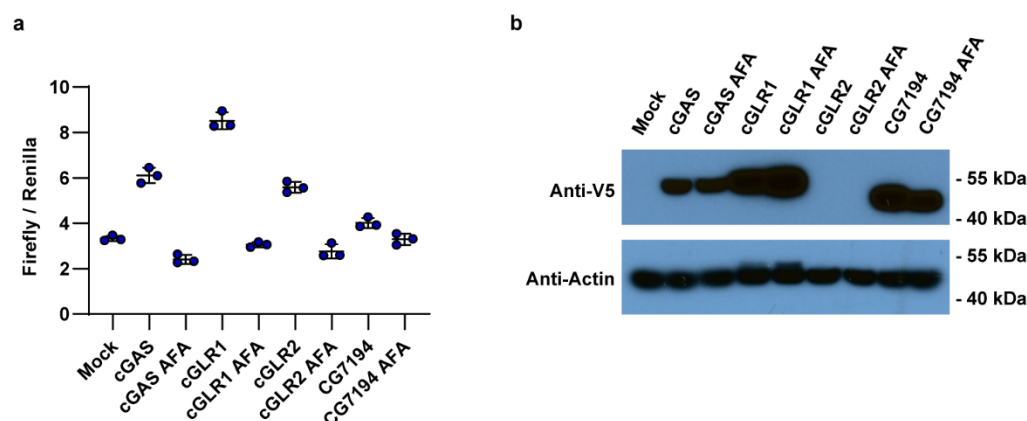
572

Extended Data Fig. 1 | Alignment of mammalian cGAS/OAS1 proteins and cGAS-like proteins from *D. melanogaster*. a, Extended view of the alignment shown in Fig. 1a with the positions of the GS/GG duplet, the metal ion coordinating acidic residues, and the Zn-finger indicated above the sequences with stars, arrows and bar, respectively. The annotated start methionine in the NCBI reference sequence for isoform D of CG30424 (cGLR2), which would delete the entire spine helix as well as part of the active site, is highlighted in yellow.



573 Deletion of the spine helix is incompatible with a folded enzyme. Furthermore, the GS-  
574 containing loop, which coordinates the  $\gamma$ -phosphate of the donor nucleotide, is a universally  
575 conserved feature of nucleotidyltransferases. **b, c**, Structure (PDB: 4K98) of murine cGAS in  
576 complex with DNA and a cGAMP intermediate analog (represented in sticks) and two  
577 magnesium ions (yellow spheres). The sidechains of the acidic active site residues and the  
578 serine in the GS motif are also represented in sticks and their oxygen atoms are colored red.  
579 Grey coloring represents the proportion of the protein upstream of the annotated start  
580 methionine site in CG30424 (cGLR2). **b**, Full view of the structure. **c**, Enhanced view of the  
581 active site.

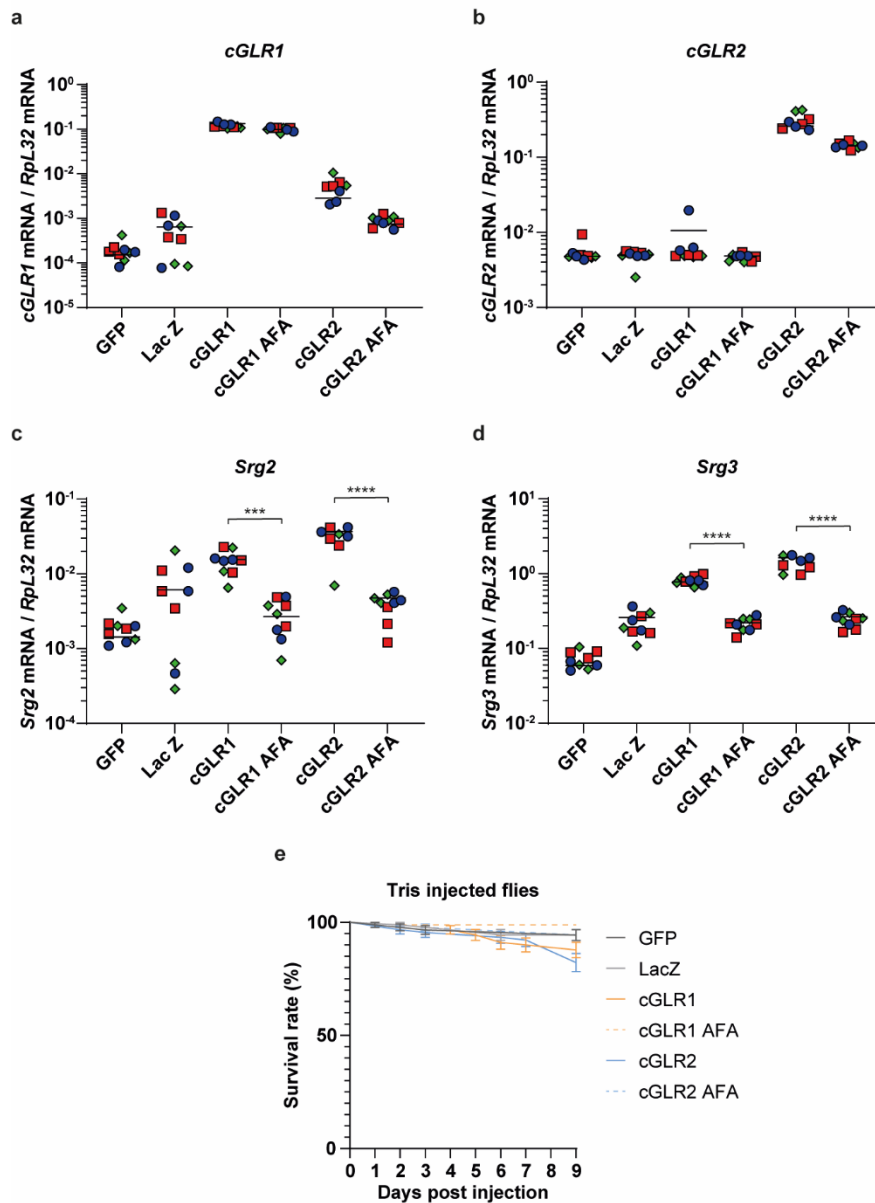
Extended Data Fig. 2 | Transient expression of cGLR1 and cGLR2 induces the Sting pathway in S2 cells



582

583 **Extended Data Fig. 2 | Transient expression of candidate cGAS-like receptors in S2**  
584 **cells. a**, Due to issues with the ANTI-FLAG® M2 antibody giving rise to non-specific bands  
585 when performing immunoblots on S2 cell lysates, we replaced the FLAG-tag we initially  
586 used with a V5-tag and reproduced the experiment from Fig. 1b. Cells were transfected with  
587 cGAS, cGLR1, cGLR2 and CG7194 or mutants thereof as well as plasmids encoding firefly  
588 or *Renilla* luciferase under transcriptional control of the *Sting* or *Actin5C* promoter,  
589 respectively. At 24 h post transfection, luciferase activity was measured. Data are from one  
590 experiment performed in triplicates and are shown with mean ± s.d. (n = 3) **b**, Immunoblot  
591 showing the expression of the V5-tagged proteins from panel (a). cGLR2 appears to be  
592 rapidly degraded in S2 cells, whereas it could easily be detected in HEK293T cells following  
593 transfection (Extended Data Fig. 10a). For gel source data, see Supplementary Fig. 1.

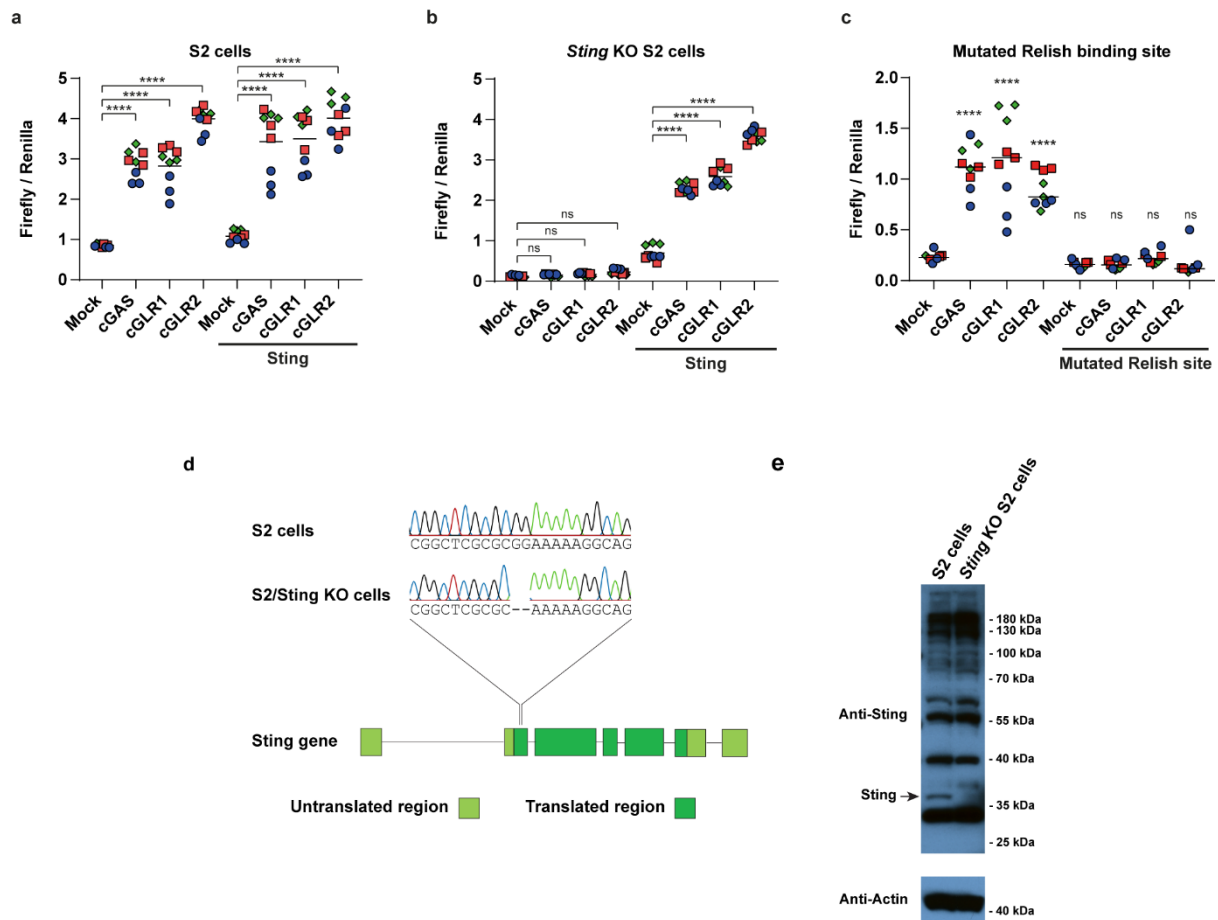
Extended Data Fig. 3 | Ectopic expression of *cGLR1* and *cGLR2* in transgenic flies induces *Srg2* and *Srg3*.



594

595 **Extended Data Fig. 3 | Ectopic expression of *cGLR1* or *cGLR2* in transgenic flies**  
 596 **induces expression of *srg2* and *srg3*.** a, b, c, d, Expression of *cGLR1* (a), *cGLR2* (b), *Srg2*  
 597 (c) and *Srg3* (d) was monitored by RT-qPCR in transgenic flies ectopically expressing wild-  
 598 type or mutant cGLRs. Expression was normalized to the housekeeping gene *RpL32*. Data are  
 599 from three independent experiments (red, blue and green, each performed in triplicate) and  
 600 shown with mean (n = 9). e, Flies of the indicated genotypes were injected with Tris and  
 601 survival was monitored daily. Data are from 3 independent experiments, each with 30 flies (n  
 602 = 90). In a, b, c, and d, data were analysed using two-way ANOVA and Holm-Šídák post hoc  
 603 test and compared to relevant AFA mutants. In e, log-rank test was used to compare *cGLR1*

604 vs. cGLR1 AFA (ns) and cGLR2 vs. cGLR2 AFA (ns). ns not significant, \*  $P < 0.05$ . \*\*  $P <$   
605  $0.01$ . \*\*\*  $P < 0.001$ .\*\*\*\*  $P < 0.0001$ .



606

607

608

609

610

611

612

613

614

615

616

617

618

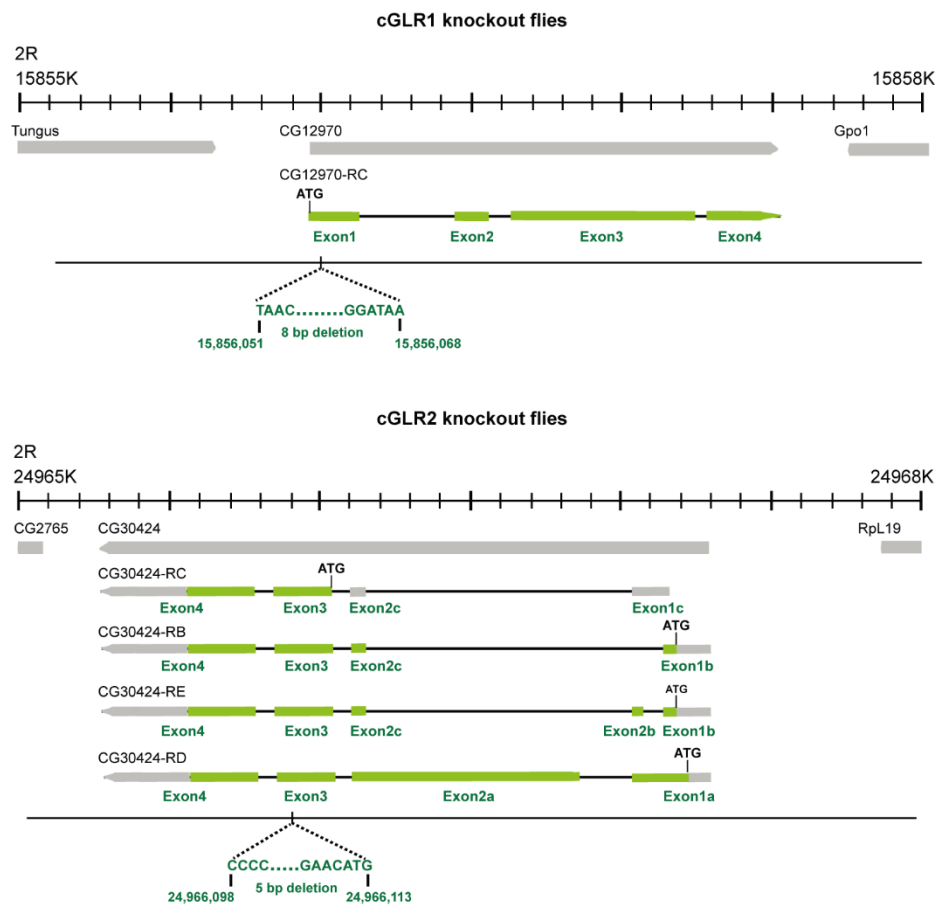
619

620

621

**Extended Data Fig. 4 | Verification of *Sting* knockout S2 cells.** S2 cells transfected with expression vectors for cGAS, cGLR1 or cGLR2 and plasmids encoding firefly or *Renilla* luciferase under transcriptional control of the *Sting* or *Actin5C* promoter, respectively, were used to monitor activation of the *Sting* pathway. **a**, S2 cells with or without co-transfection with an expression vector for *Sting*. **b**, *Sting* knockout (KO) S2 cells with or without co-transfection with an expression vector for *Sting*. **c**, S2 cells transfected with expression vectors for cGAS, cGLR1 or cGLR2 and plasmid encoding firefly luciferase under transcriptional control of the *Sting* promoter or a mutated version containing two point mutations in the Relish binding site. Data are from three independent experiments (blue, red, and green, each performed in triplicates) and are shown with mean ( $n = 9$ ). Data were analyzed using two-way ANOVA and Holm-Šidák post hoc test and compared to mock. ns not significant, \*\*\*\*  $P < 0.0001$ . **d**, Sanger sequencing showing the 2 bp deletion in the *Sting* gene in *Sting* knockout (KO) S2 cells. **e**, Immunoblot showing the lack of expression of *Sting* in *Sting* KO S2 cells. The arrow indicates the position of the *Sting* band. For gel source data, see Supplementary Fig. 1.

Extended Data Fig. 5 | Generation of *cGLR1* and *cGLR2* knockout flies



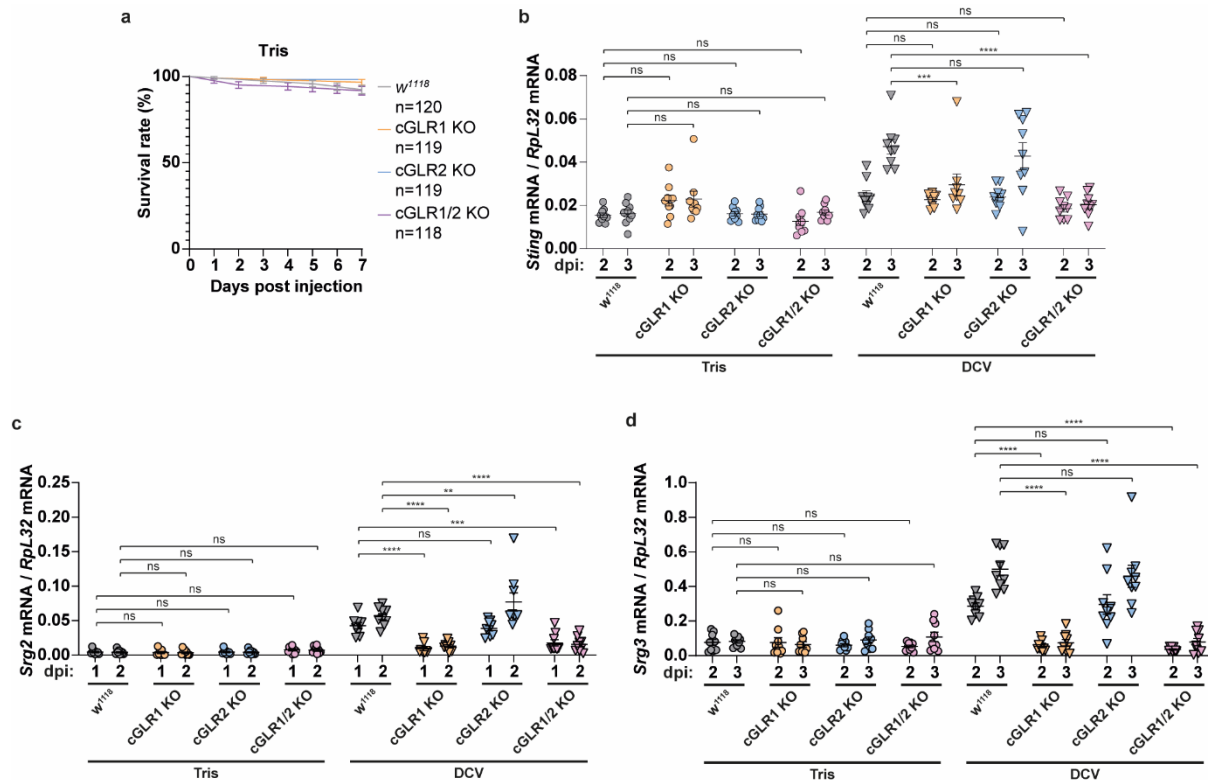
622

623 **Extended Data Fig. 5 | Generation of *cGLR1* and *cGLR2* knockout flies.** The *cGLR1* and  
 624 *cGLR2* genes, both located on the right arm of the second chromosome, are shown together  
 625 with their annotated transcripts. Open reading frames are indicated in green. For *cGLR1*, an 8  
 626 bp deletion was introduced in the first exon using CRISPR/Cas9 technology. The deletion  
 627 creates a frameshift after the asparagine residue at position 31, leading to termination of  
 628 translation after insertion of single glycine residue. For *cGLR2*, a 5 bp deletion was created in  
 629 exon 3, which is shared by all isoforms. The deletion results in a frameshift after the  
 630 glutamate residue at position 338, leading to termination of translation after insertion of a 32  
 631 amino acid extension (HDDRIDPGSSLGNVPVRAKDSKRPEGRRDQPE).

632

633





634

635

**Extended Data Fig. 6 | Expression of *Sting*, *Srg2* and *Srg3* in flies upon infection with**

636

**DCV. a**, Corresponding control to Fig. 2a.  $w^{1118}$ , cGLR1 KO, cGLR2 KO or cGLR1/2 KO

637

flies were injected with Tris and survival was monitored daily. Data are from three

638

independent experiments, each with three groups of around 10 flies. **b**, **c**, **d**,  $w^{1118}$ , cGLR1

639

KO, cGLR2 KO or cGLR1/2 KO flies were injected with DCV or Tris and expression of

640

*Sting* (**a**), *Srg2* (**b**) and *Srg3* (**c**) was monitored by RT-qPCR at 2 and 3 days post-infection

641

(dpi). Expression was normalized to the housekeeping gene *RpL32*. Data are from three

642

independent experiments, each performed in triplicates (n = 9). In a, log-rank test was used to

643

test if the survival curves differed. In **b**, **c** and **d**, data were analyzed using two-way ANOVA

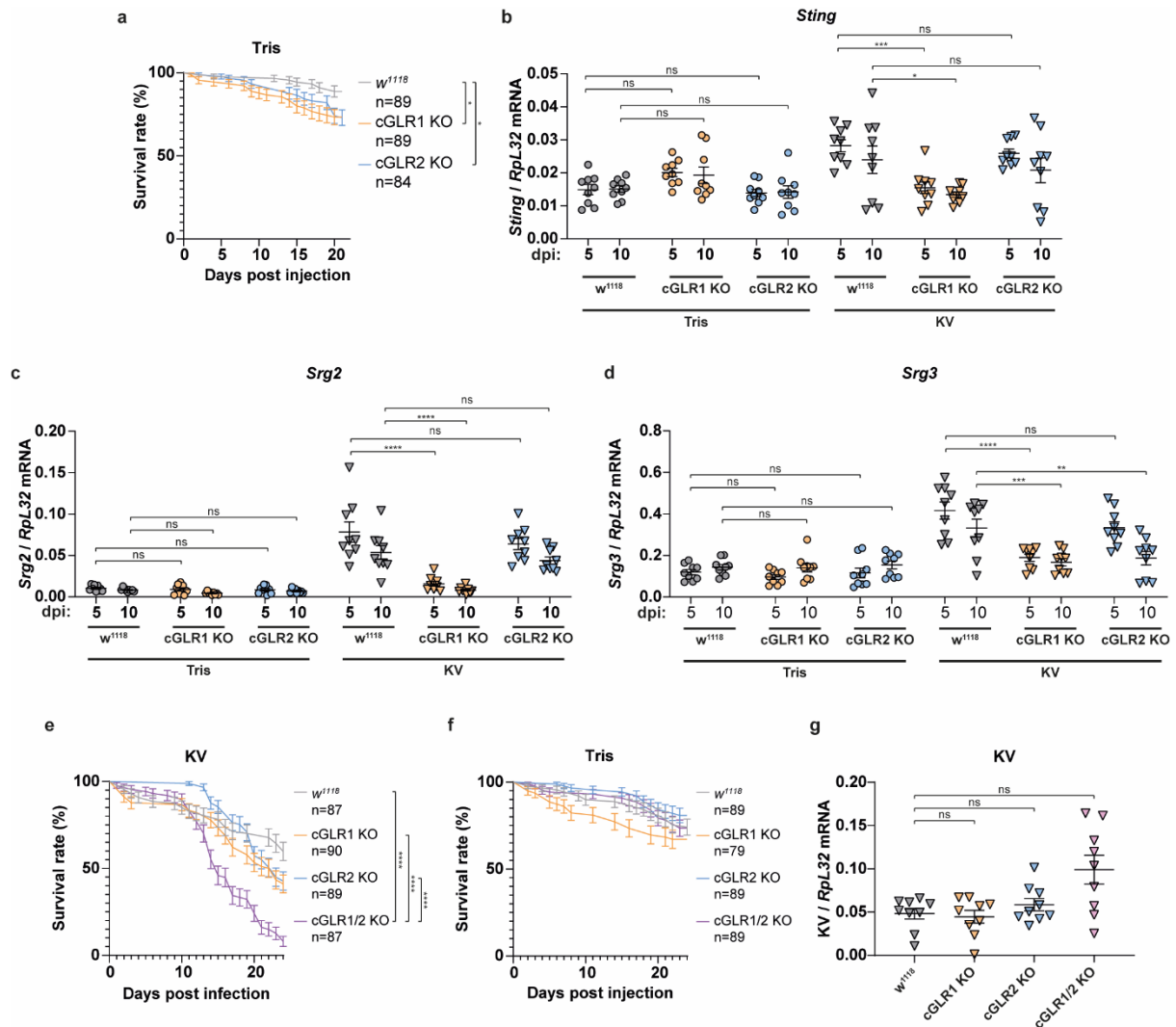
644

and Holm-Šídák post hoc test and compared to  $w^{1118}$  flies. ns not significant, \*\*  $P < 0.01$ . \*\*\*

645

$P < 0.001$ . \*\*\*\*  $P < 0.0001$ .

646



647

648 **Extended Data Fig. 7 | Expression of *Sting*, *Srg2* and *Srg3* in flies upon infection with**  
 649 **KV.** **a**, Corresponding control to Fig. 2b.  $w^{1118}$ , cGLR1 KO or cGLR2 KO flies were injected  
 650 with Tris and survival was monitored daily. Data are from three independent experiments,  
 651 each with three groups of around 10 flies. **b**, **c**, **d**,  $w^{1118}$ , cGLR1 KO or cGLR2 KO flies were  
 652 injected with KV or Tris and expression of *Sting* (**a**), *Srg2* (**b**) and *Srg3* (**c**) was monitored by  
 653 RT-qPCR at 5 and 10 days post-infection (dpi). Expression was normalized to the  
 654 housekeeping gene *RpL32*. Data are from three independent experiments, each performed  
 655 in triplicates ( $n = 9$ ). **e**, **f**,  $w^{1118}$ , cGLR1 KO, cGLR2 KO or cGLR1/2 KO flies were injected  
 656 with KV (**e**) or Tris (**f**) and survival was monitored daily. Data are from three independent  
 657 experiments, each with three groups of around 10 flies. **g**,  $w^{1118}$ , cGLR1 KO, cGLR2 or  
 658 cGLR1/2 KO flies were injected with KV and viral load was monitored by RT-qPCR at 5  
 659 days post-infection (dpi). Expression was normalized to the housekeeping gene *RpL32*. Data  
 660 are from three independent experiments, each performed in triplicates ( $n = 9$ ). In **a**, **e**, **f**, log-

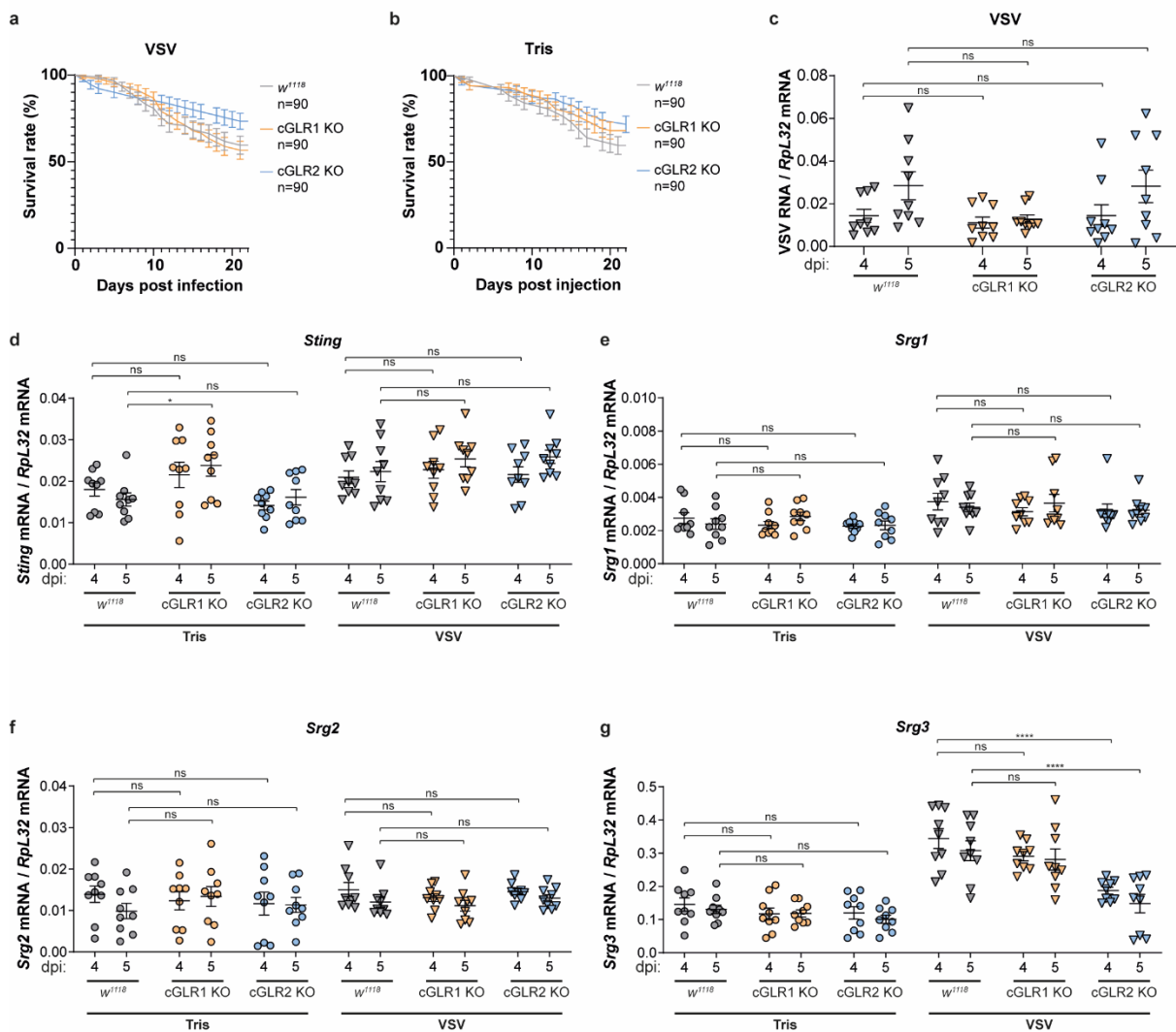
661 rank test was used to compare the survival curves pairwise followed by a Holm-Šídák  
 662 multiple comparison correction. In **b**, **c** and **d**, data were analyzed using two-way ANOVA  
 663 and Holm-Šídák post hoc test and compared to  $w^{1118}$  flies. In **g**, Log transformed data were  
 664 analyzed using one-way ANOVA and Dunnett T3 post hoc test and compared to  $w^{1118}$  flies.  
 665 ns not significant, \*\*  $P < 0.01$ . \*\*\*  $P < 0.001$ . \*\*\*\*  $P < 0.0001$ .

666

667

668

Extended Data Fig 7 | Loss of cGFR1 or cGFR2 has a limited effect on VSV infection in flies



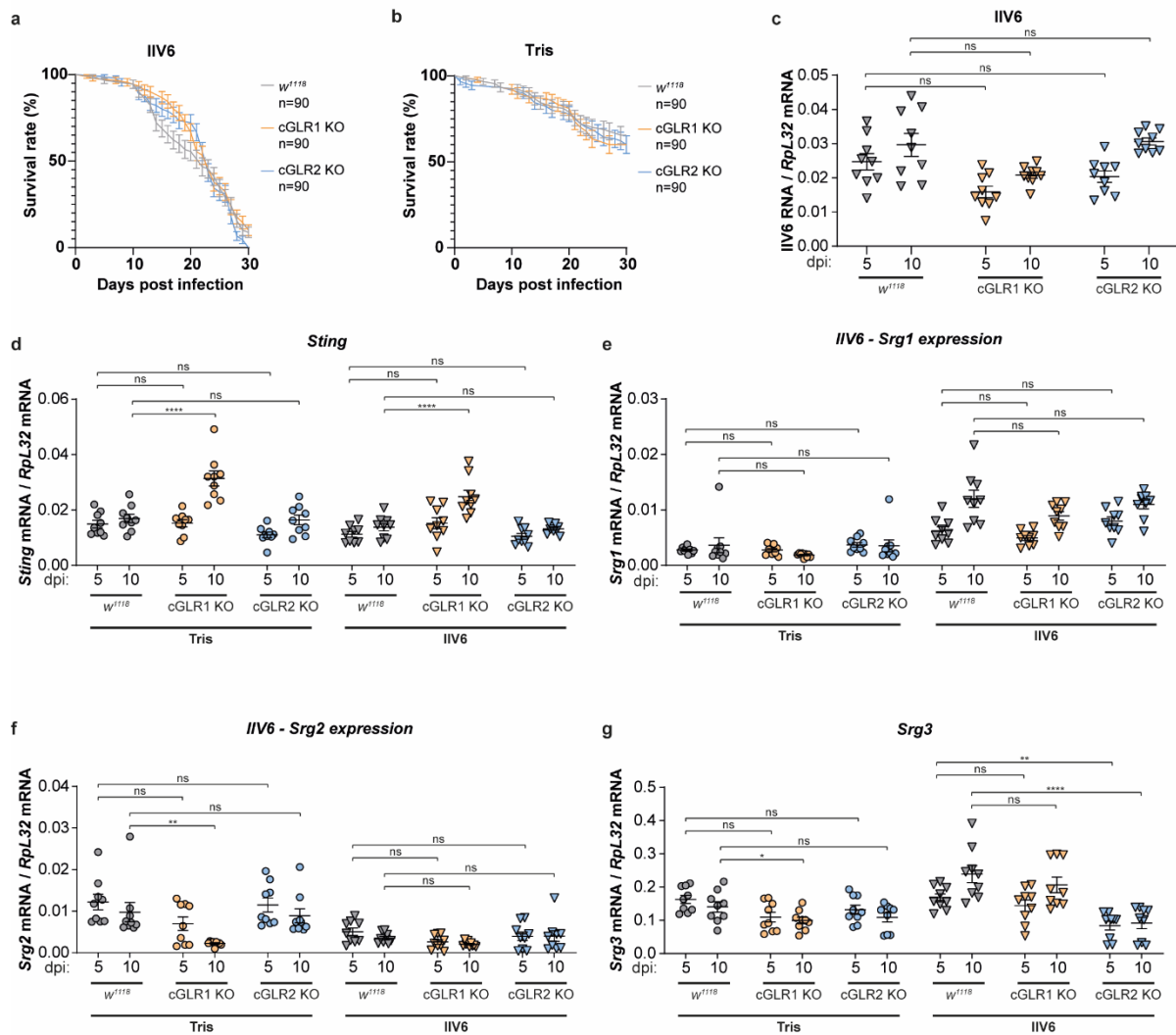
669

670

671

Extended Data Fig. 8 | Loss of cGFR1 or cGFR2 has a limited effect on VSV infection in flies. **a**, **b**,  $w^{1118}$ , cGFR1 KO or cGFR2 KO flies were injected with VSV (**a**) or Tris (**b**) and

672 survival was monitored daily. Data are from three independent experiments, each with three  
673 groups of around 10 flies. **c, d, e, f, g**,  $w^{1118}$ , cGLR1 KO, cGLR2 KO or cGLR1/2 KO flies  
674 were injected with VSV or Tris and viral load (**c**) as well as expression of *Sting* (**d**), *Srg1* (**e**),  
675 *Srg2* (**f**) and *Srg3* (**g**) were monitored by RT-qPCR at 4 and 5 days post-infection (dpi).  
676 Expression was normalized to the housekeeping gene *RpL32*. Data are from three  
677 independent experiments, each performed in triplicates (n = 9). In **a** and **b**, log-rank test was  
678 used to test if the survival curves differed. In **c**, Log transformed data were analyzed using  
679 one-way ANOVA and Dunnett T3 post hoc test and compared to  $w^{1118}$  flies. In **d, e, f** and **g**,  
680 data were analyzed using two-way ANOVA and Holm-Šídák post hoc test and compared to  
681  $w^{1118}$  flies. ns not significant, \*  $P < 0.05$ . \*\*\*  $P < 0.001$ . \*\*\*\*  $P < 0.0001$ .



682

683

684

685

686

687

688

689

690

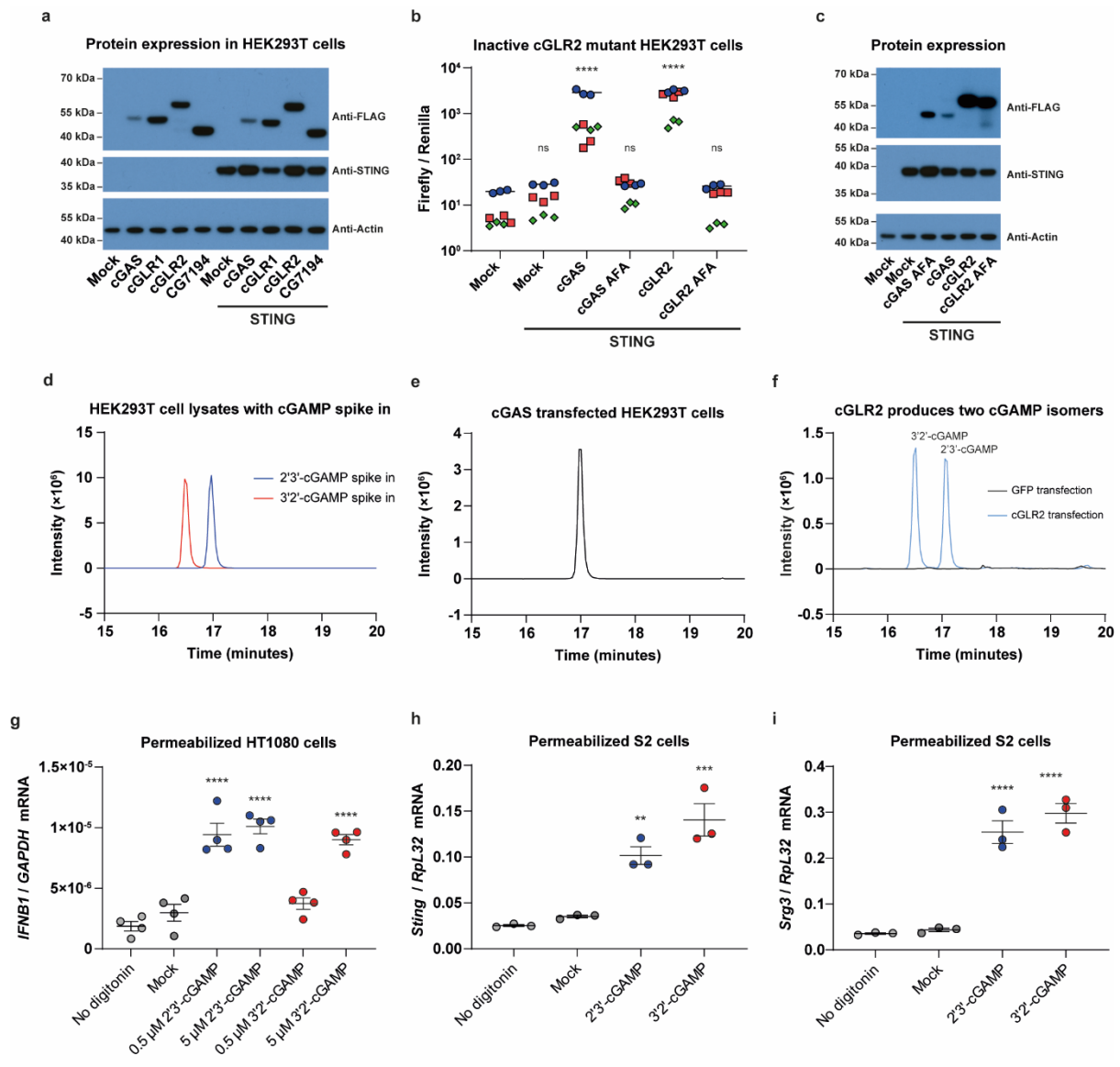
691

692

693

694

**Extended Data Fig. 9 | Loss of cGLR1 or cGLR2 has a limited effect on IIV6 infection in flies.** **a, b,**  $w^{1118}$ , cGLR1 KO or cGLR2 KO flies were injected with IIV6 (**a**) or Tris (**b**) and survival was monitored daily. Data are from three independent experiments, each with three groups of around 10 flies. **c, d, e, f, g,**  $w^{1118}$ , cGLR1 KO or cGLR2 KO flies were injected with IIV6 or Tris and viral load (**c**) as well as expression of *Sting* (**d**), *Srg1* (**e**), *Srg2* (**f**) and *Srg3* (**g**) were monitored by RT-qPCR at 5 and 10 days post-infection (dpi). Expression was normalized to the housekeeping gene *RpL32*. Data are from three independent experiments, each performed in triplicates ( $n = 9$ ). In **a** and **b**, log-rank test was used to test if the survival curves differed. In **c**, Log transformed data were analyzed using one-way ANOVA and Dunnett T3 post hoc test and compared to  $w^{1118}$  flies. In **d, e, f** and **g**, data were analyzed using two-way ANOVA and Holm-Šidák post hoc test and compared to  $w^{1118}$  flies. ns not significant, \*  $P < 0.05$ . \*\*  $P < 0.01$ . \*\*\*  $P < 0.001$ . \*\*\*\*  $P < 0.0001$ .



695

696

697

698

699

700

701

702

703

704

705

706

707

**Extended Data Fig. 10 | cGRL2 produce 2'3'-cGAMP and 3'2'-cGAMP, which can activate human and *Drosophila* STING.** **a**, Immunoblot showing the expression of STING and FLAG-tagged nucleotidyltransferases from Fig. 3a. **b**, HEK293T cells transfected with cGAS, cGAS AFA, cGRL2, cGRL2 AFA, and STING as indicated and plasmids encoding firefly or *Renilla* luciferase under transcriptional control of the *IFNβ1* or a constitutive promoter, respectively. Data are from three independent experiments (blue, red, and green, each performed in triplicates) and shown with mean (n = 9). **c**, Immunoblot showing the expression of STING and FLAG-tagged nucleotidyltransferases from panel (b). **d**, Representative chromatograms from mass spectrometry analysis of 2'3'-cGAMP or 3'2'-cGAMP spiked lysates from GFP transfected cells. **e**, Representative chromatogram from mass spectrometry analysis of cGAS transfected cells. **f**, Representative chromatograms from mass spectrometry analysis of GFP or cGRL2 transfected cells. **g**, **h**, **i**, HT-1080 (**g**) or S2

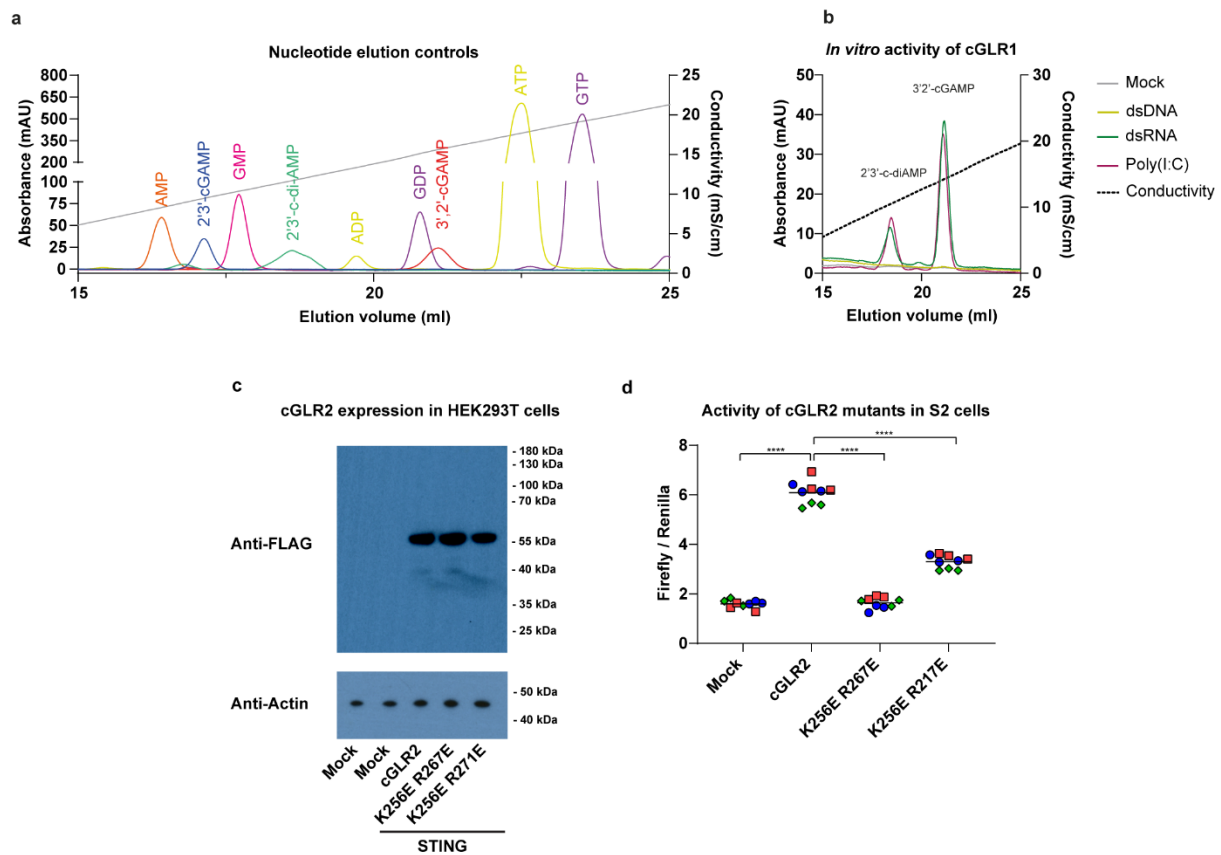
708 cells (**h** and **i**) permeabilized using digitonin and treated with the indicated cGAMPs.  
709 Expression of *IFNB1* (**g**), *Sting* (**h**) or *Srg1* (**i**) were monitored by RT-qPCR at 6 and 8 h post  
710 treatment for S2 and HT-1080 cells, respectively. Expression was normalized to the  
711 housekeeping genes GAPDH (**g**) and *RpL32* (**h** and **i**). Data are shown with mean  $\pm$  s.e.m. (n  
712 = 4 for **g** and n = 3 for **h** and **i**). In **b**, data were analyzed using two-way ANOVA and Holm-  
713 Šídák and compared to mock. In **g**, **h**, **i**, data were analyzed using one-way ANOVA and  
714 Dunnett T3 post hoc test and compared to mock. ns not significant, \*\*  $P < 0.01$ . \*\*\*  $P <$   
715 0.001. \*\*\*\*  $P < 0.0001$ .

716

717

718





719

720

721

722

723

724

725

726

727

728

729

730

731

732

**Extended Data Fig. 11 | cGRL1 produces 3'2'-cGAMP in response to dsRNA. a,** Representative chromatograms from anion exchange chromatography analysis of different nucleotides. **b,** Representative chromatograms from anion exchange chromatography analysis of reaction products from activity assays with recombinant cGRL1 in the presence of different nucleic acids. **c,** Immunoblot showing the expression of FLAG-tagged cGRL2 and mutants thereof from Fig. 3f. **d,** S2 cells transfected with cGRL2 or mutants thereof as well as plasmids encoding firefly or *Renilla* luciferase under transcriptional control of the *Sting* or *Actin5C* promoter, respectively. Data are from three independent experiments (blue, red, and green, each performed in triplicates) and shown with mean (n = 9). In **d,** data were analyzed using two-way ANOVA and Holm-Šídák post hoc test and compared to cGRL2. ns not significant, \*\*\*\*  $P < 0.0001$ .

734

735

736

737

738

739

740

741

742

743

744

745

746

747

748

749

750

751

752

753

754

755

756

757

758

759

760

761

762

763

764

765

766

767

768

769

770

771

772

773

774

775

776

777

778

779

780

781

- 1 Whiteley, A. T. *et al.* Bacterial cGAS-like enzymes synthesize diverse nucleotide signals. *Nature* **567**, 194-199, doi:10.1038/s41586-019-0953-5 (2019).
- 2 Ablasser, A. *et al.* cGAS produces a 2'-5'-linked cyclic dinucleotide second messenger that activates STING. *Nature* **498**, 380-384, doi:10.1038/nature12306 (2013).
- 3 Civril, F. *et al.* Structural mechanism of cytosolic DNA sensing by cGAS. *Nature* **498**, 332-337, doi:10.1038/nature12305 (2013).
- 4 Sun, L., Wu, J., Du, F., Chen, X. & Chen, Z. J. Cyclic GMP-AMP synthase is a cytosolic DNA sensor that activates the type I interferon pathway. *Science* **339**, 786-791, doi:10.1126/science.1232458 (2013).
- 5 Wu, J. *et al.* Cyclic GMP-AMP is an endogenous second messenger in innate immune signaling by cytosolic DNA. *Science* **339**, 826-830, doi:10.1126/science.1229963 (2013).
- 6 Lowey, B. *et al.* CBASS Immunity Uses CARF-Related Effectors to Sense 3'-5'- and 2'-5'-Linked Cyclic Oligonucleotide Signals and Protect Bacteria from Phage Infection. *Cell* **182**, 38-49 e17, doi:10.1016/j.cell.2020.05.019 (2020).
- 7 Morehouse, B. R. *et al.* STING cyclic dinucleotide sensing originated in bacteria. *Nature* **586**, 429-433, doi:10.1038/s41586-020-2719-5 (2020).
- 8 Cohen, D. *et al.* Cyclic GMP-AMP signalling protects bacteria against viral infection. *Nature* **574**, 691-695, doi:10.1038/s41586-019-1605-5 (2019).
- 9 Guo, Z., Li, Y. & Ding, S. W. Small RNA-based antimicrobial immunity. *Nature reviews. Immunology* **19**, 31-44, doi:10.1038/s41577-018-0071-x (2019).
- 10 Schneider, J. & Imler, J. L. Sensing and signalling viral infection in drosophila. *Dev Comp Immunol* **117**, 103985, doi:10.1016/j.dci.2020.103985 (2021).
- 11 Goto, A. *et al.* The Kinase IKKbeta Regulates a STING- and NF-kappaB-Dependent Antiviral Response Pathway in Drosophila. *Immunity* **49**, 225-234 e224, doi:10.1016/j.immuni.2018.07.013 (2018).
- 12 Liu, Y. *et al.* Inflammation-Induced, STING-Dependent Autophagy Restricts Zika Virus Infection in the Drosophila Brain. *Cell Host Microbe* **24**, 57-68 e53, doi:10.1016/j.chom.2018.05.022 (2018).
- 13 Hua, X. *et al.* Stimulator of interferon genes (STING) provides insect antiviral immunity by promoting Dredd caspase-mediated NF-kappaB activation. *J Biol Chem* **293**, 11878-11890, doi:10.1074/jbc.RA117.000194 (2018).
- 14 Donelick, H. M. *et al.* In vitro studies provide insight into effects of Dicer-2 helicase mutations in Drosophila melanogaster. *RNA* **26**, 1847-1861, doi:10.1261/rna.077289.120 (2020).
- 15 Jin, L. *et al.* MPYS is required for IFN response factor 3 activation and type I IFN production in the response of cultured phagocytes to bacterial second messengers cyclic-di-AMP and cyclic-di-GMP. *J Immunol* **187**, 2595-2601, doi:10.4049/jimmunol.1100088 (2011).
- 16 Burdette, D. L. *et al.* STING is a direct innate immune sensor of cyclic di-GMP. *Nature* **478**, 515-518, doi:10.1038/nature10429 (2011).
- 17 Diner, E. J. *et al.* The innate immune DNA sensor cGAS produces a noncanonical cyclic dinucleotide that activates human STING. *Cell Rep* **3**, 1355-1361, doi:10.1016/j.celrep.2013.05.009 (2013).
- 18 Gao, P. *et al.* Cyclic [G(2',5')pA(3',5')p] is the metazoan second messenger produced by DNA-activated cyclic GMP-AMP synthase. *Cell* **153**, 1094-1107, doi:10.1016/j.cell.2013.04.046 (2013).

- 782 19 Kranzusch, P. J., Lee, A. S., Berger, J. M. & Doudna, J. A. Structure of human cGAS  
783 reveals a conserved family of second-messenger enzymes in innate immunity. *Cell*  
784 *Rep* **3**, 1362-1368, doi:10.1016/j.celrep.2013.05.008 (2013).
- 785 20 Zhang, X. *et al.* Cyclic GMP-AMP containing mixed phosphodiester linkages is an  
786 endogenous high-affinity ligand for STING. *Mol Cell* **51**, 226-235,  
787 doi:10.1016/j.molcel.2013.05.022 (2013).
- 788 21 Cai, H. *et al.* 2'3'-cGAMP triggers a STING- and NF-kappaB-dependent broad  
789 antiviral response in Drosophila. *Sci Signal* **13**, doi:10.1126/scisignal.abc4537 (2020).
- 790 22 Wu, X. *et al.* Molecular evolutionary and structural analysis of the cytosolic DNA  
791 sensor cGAS and STING. *Nucleic Acids Res* **42**, 8243-8257, doi:10.1093/nar/gku569  
792 (2014).
- 793 23 Martin, M., Hiroyasu, A., Guzman, R. M., Roberts, S. A. & Goodman, A. G. Analysis  
794 of Drosophila STING Reveals an Evolutionarily Conserved Antimicrobial Function.  
795 *Cell Rep* **23**, 3537-3550 e3536, doi:10.1016/j.celrep.2018.05.029 (2018).
- 796 24 Caygill, E. E. & Brand, A. H. The GAL4 System: A Versatile System for the  
797 Manipulation and Analysis of Gene Expression. *Methods Mol Biol* **1478**, 33-52,  
798 doi:10.1007/978-1-4939-6371-3\_2 (2016).
- 799 25 Tanaka, Y. & Chen, Z. J. STING specifies IRF3 phosphorylation by TBK1 in the  
800 cytosolic DNA signaling pathway. *Sci Signal* **5**, ra20, doi:10.1126/scisignal.2002521  
801 (2012).
- 802 26 Zhong, B. *et al.* The adaptor protein MITA links virus-sensing receptors to IRF3  
803 transcription factor activation. *Immunity* **29**, 538-550,  
804 doi:10.1016/j.immuni.2008.09.003 (2008).
- 805 27 Palmer, W. H., Medd, N. C., Beard, P. M. & Obbard, D. J. Isolation of a natural DNA  
806 virus of Drosophila melanogaster, and characterisation of host resistance and immune  
807 responses. *PLoS Pathog* **14**, e1007050, doi:10.1371/journal.ppat.1007050 (2018).
- 808 28 Slavik, K. M. *et al.* cGAS-like receptors control RNA sensing and 3'2'-cGAMP  
809 antiviral signaling in Drosophila. *Under consideration at Nature* (2021).
- 810 29 Hartmann, R., Justesen, J., Sarkar, S. N., Sen, G. C. & Yee, V. C. Crystal structure of  
811 the 2'-specific and double-stranded RNA-activated interferon-induced antiviral  
812 protein 2'-5'-oligoadenylate synthetase. *Mol Cell* **12**, 1173-1185, doi:10.1016/s1097-  
813 2765(03)00433-7 (2003).
- 814 30 Gui, X. *et al.* Autophagy induction via STING trafficking is a primordial function of  
815 the cGAS pathway. *Nature* **567**, 262-266, doi:10.1038/s41586-019-1006-9 (2019).
- 816 31 McFarland, A. P. *et al.* Sensing of Bacterial Cyclic Dinucleotides by the  
817 Oxidoreductase RECON Promotes NF-kappaB Activation and Shapes a  
818 Proinflammatory Antibacterial State. *Immunity* **46**, 433-445,  
819 doi:10.1016/j.immuni.2017.02.014 (2017).
- 820 32 Eaglesham, J. B., McCarty, K. L. & Kranzusch, P. J. Structures of diverse poxins  
821 cGAMP nucleases reveal a widespread role for cGAS-STING evasion in host-  
822 pathogen conflict. *Elife* **9**, doi:10.7554/eLife.59753 (2020).
- 823 33 Eaglesham, J. B., Pan, Y., Kupper, T. S. & Kranzusch, P. J. Viral and metazoan  
824 poxins are cGAMP-specific nucleases that restrict cGAS-STING signalling. *Nature*  
825 **566**, 259-263, doi:10.1038/s41586-019-0928-6 (2019).
- 826 34 Hernaez, B. *et al.* Viral cGAMP nuclease reveals the essential role of DNA sensing in  
827 protection against acute lethal virus infection. *Sci Adv* **6**, doi:10.1126/sciadv.abb4565  
828 (2020).
- 829 35 Lowey, B. & Kranzusch, P. J. CD-NTases and nucleotide second messenger  
830 signaling. *Curr Biol* **30**, R1106-R1108, doi:10.1016/j.cub.2020.06.096 (2020).

- 831 36 Andersen, L. L. *et al.* Frequently used bioinformatics tools overestimate the damaging  
832 effect of allelic variants. *Genes Immun* **20**, 10-22, doi:10.1038/s41435-017-0002-z  
833 (2019).
- 834 37 Andersen, L. L. *et al.* Functional IRF3 deficiency in a patient with herpes simplex  
835 encephalitis. *J Exp Med* **212**, 1371-1379, doi:10.1084/jem.20142274 (2015).
- 836 38 Schulz, A., Jankowski, V., Zidek, W. & Jankowski, J. Highly sensitive, selective and  
837 rapid LC-MS method for simultaneous quantification of diadenosine polyphosphates  
838 in human plasma. *J Chromatogr B Analyt Technol Biomed Life Sci* **961**, 91-96,  
839 doi:10.1016/j.jchromb.2014.05.018 (2014).
- 840 39 Wang, Y., Holleufer, A., Gad, H. H. & Hartmann, R. Length dependent activation of  
841 OAS proteins by dsRNA. *Cytokine* **126**, 154867, doi:10.1016/j.cyto.2019.154867  
842 (2020).
- 843 40 Holleufer, A. & Hartmann, R. A Highly Sensitive Anion Exchange Chromatography  
844 Method for Measuring cGAS Activity in vitro. *Bio-protocol* **8**, e3055,  
845 doi:10.21769/BioProtoc.3055 (2018).  
846